Title

Hypersensitivity to Distractors in Fragile X Syndrome from Loss of Modulation of Cortical VIP Interneurons.

Journal

Journal of Neuroscience, 43(48)

Authors

Rahmatullah, Noorhan
Schmitt, Lauren
De Stefano, Lisa
et al.

Publication Date

2023-11-29

DOI

10.1523/JNEUROSCI.0571-23.2023

Systems/Circuits

Hypersensitivity to Distractors in Fragile X Syndrome from Loss of Modulation of Cortical VIP Interneurons

Noorhan Rahmatullah,[1,2*] Lauren M. Schmitt,[7,8*] Lisa De Stefano,[3] Sam Post,[2] Jessica Robledo,[2] Gunvant Chaudhari,[5] Ernest Pedapati,[3,4] Craig Erickson,[3] Carlos Portera-Cailliau,[5,6] and Anubhuti Goel[1,2]

[1]Neuroscience Graduate Program, University of California, Riverside, Riverside, California 92521, [2]Department of Psychology, University of California, Riverside, Riverside, California 92521, [3]Department of Psychiatry, Cincinnati Children's Hospital Medical Center, University of Cincinnati College of Medicine, Cincinnatti, Ohio 45267, [4]Department of Neurology, Cincinnati Children's Hospital Medical Center, University of Cincinnati College of Medicine, Cincinnatti, Ohio 45267, [5]Department of Neurology, David Geffen School of Medicine, University of California, Los Angeles, Los Angeles, California 90095, [6]Department of Neurobiology, David Geffen School of Medicine, University of California, Los Angeles, Los Angeles, California 90095, [7]Division of Behavioral Medicine and Clinical Psychology, Cincinnati Children's Hospital Medical Center, Cincinnati, OH 45229, and [8]Department of Pediatrics, University of Cincinnati College of Medicine, Cincinnati OH 45267

Attention deficit is one of the most prominent and disabling symptoms in Fragile X syndrome (FXS). Hypersensitivity to sensory stimuli contributes to attention difficulties by overwhelming and/or distracting affected individuals, which disrupts activities of daily living at home and learning at school. We find that auditory or visual distractors selectively impair visual discrimination performance in humans and mice with FXS but not in typically developing controls. In both species, males and females were examined. Vasoactive intestinal polypeptide (VIP) neurons were significantly modulated by incorrect responses in the poststimulus period during early distractor trials in WT mice, consistent with their known role as error signals. Strikingly, however, VIP cells from *Fmr1*$^{-/-}$ mice showed little modulation in error trials, and this correlated with their poor performance on the distractor task. Thus, VIP interneurons and their reduced modulatory influence on pyramidal cells could be a potential therapeutic target for attentional difficulties in FXS.

Key words: **attention-deficit disorder; autism spectrum disorders; calcium imaging; *Fmr1* knockout; inhibition; VIP**

Significance Statement

Sensory hypersensitivity, impulsivity, and persistent inattention are among the most consistent clinical features of FXS, all of which impede daily functioning and create barriers to learning. However, the neural mechanisms underlying sensory over-reactivity remain elusive. To overcome a significant challenge in translational FXS research we demonstrate a compelling alignment of sensory over-reactivity in both humans with FXS and *Fmr1*$^{-/-}$ mice (the principal animal model of FXS) using a novel analogous distractor task. Two-photon microscopy in mice revealed that lack of modulation by VIP cells contributes to susceptibility to distractors. Implementing research efforts we describe here can help identify dysfunctional neural mechanisms associated not only with sensory issues but broader impairments, including those in learning and cognition.

Introduction

Fragile X syndrome (FXS), the most common inherited form of intellectual disability, is associated with several comorbid conditions, such as epilepsy, anxiety, aggression, autism, and sensory hypersensitivity (Bailey et al., 2008). The focus of basic and translational research efforts in animal models of FXS has been placed on investigating neural mechanisms associated with these symptoms. Behaviorally speaking, however, the most consistent feature of FXS children is their persistent inattention, impulsivity, fidgetiness, and restlessness, with most individuals

Received Mar. 29, 2023; revised Aug. 11, 2023; accepted Sep. 14, 2023.

Author contributions: L.M.S., E.P., C.E., C.P.-C., and A.G. designed research; N.R., L.M.S., L.D., J.R., and G.C. performed research; N.R., S.P., and A.G. analyzed data; A.G. wrote the paper.

This work was supported by the National Institutes of Health–National Institute of Neurological Disorders and Stroke Grants R01NS117597 and R01HD054453, U.S. Department of Defense Grant 13196175 (C.P.-C.), and Brain and Behavior Young Investigator Award (A.G.). We thank Nazim Kourdougli and Trishala Chari for help with behavioral studies; the individuals with FXS, their families, and the controls who participated in this study; the clinical research coordinators for assistance with data collection and data entry as well as the basic laboratory research assistants for work on the FMRP (Fragile X messenger ribonucleoprotein); and Elizabeth Berry-Kravis at Rush University for testing for *FMR1* gene CGG expansion and gene methylation.

G. Chaudhari's present address: University of California, San Francisco, School of Medicine, 400 Parnassus Avenue, San Francisco, California 94143.

*N.R. and L.M.S. contributed equally to this work.

The authors declare no competing interests.

Correspondence should be addressed to Anubhuti Goel at anubhuti.goel@ucr.edu or Carlos Portera-Cailliau at cpcailliau@mednet.ucla.edu.

https://doi.org/10.1523/JNEUROSCI.0571-23.2023

with FXS meeting criteria for a diagnosis of attention deficit hyperactivity disorder (ADD), particularly the inattentive type (Sullivan et al., 2006; Grefer et al., 2016). At the same time, individuals with FXS experience prominent sensory over-responsivity (SOR), which is characterized by exaggerated responses to certain auditory, visual, olfactory, and tactile stimuli that are innocuous to neurotypical individuals (Miller et al., 1999; Cornish et al., 2004; Van der Molen et al., 2012; Sinclair et al., 2017; Rais et al., 2018). Sometimes referred to as a sensory-modulation disorder, SOR triggers maladaptive behaviors in FXS, such as avoidance, defensive responses, or distraction and inattention (consistent with comorbid diagnosis of attention deficit hyperactivity disorder), which in turn contributes to learning deficits (Kogan et al., 2004; Kaufmann et al., 2017).

Remarkably, despite the prevalence and importance of attentional difficulties in FXS, it has been understudied in animal models. Its underlying neural mechanisms and how they might interfere with learning and cognition are largely unknown. It has long been proposed that neuropsychiatric symptoms in FXS and other neurodevelopmental conditions (NDCs) are linked to hyperexcitability and reduced GABAergic inhibition (Rubenstein and Merzenich, 2003; Contractor et al., 2015, 2021). In FXS, SOR and attentional difficulties likely engage complex interactions between excitatory neurons and several interneuron subclasses, yet these circuit dynamics have not been explored in detail during behavior.

Previously, we reported that *Fmr1*$^{-/-}$ mice, the best-studied animal model of FXS (Dutch-Belgian Fragile X Consortium, 1994), exhibit impairments on a go/no-go visual discrimination task compared with wild-type (WT) controls—a deficit that was recapitulated in humans with FXS (Goel et al., 2018). Accurate performance in such a task requires the animal to attend to task-relevant information and ignore task-irrelevant information (i.e., sensory distractors; Baluch and Itti, 2011; Zhang et al., 2014). Because *Fmr1*$^{-/-}$ mice exhibit SOR (Chen and Toth, 2001; Rotschafer and Razak, 2013, 2014; He et al., 2017), just like people with FXS, we hypothesized that they would be unable to tune out sensory distractors, and this would have a negative impact on their performance on the visual task.

Thus, we set out to investigate the intersection of attentional difficulties, SOR, and perceptual decision-making in FXS, and the underlying neural mechanisms using a visual discrimination task. We show that sensory distractors selectively impaired task performance in both *Fmr1*$^{-/-}$ mice and FXS humans. Calcium imaging in primary visual cortex (V1) showed that vasoactive intestinal polypeptide (VIP) cell activity was less modulated by visual stimuli in task-naive *Fmr1*$^{-/-}$ mice than in WT controls. Moreover, in distractor trials, VIP cells were modulated by incorrect responses in WT mice in early sessions, whereas in *Fmr1*$^{-/-}$ mice VIP cells lacked such modulation. In fact, VIP cell modulation was correlated with the speed of perceptual learning and the ability to tune out sensory distractors.

Materials and Methods

Experimental animals

All experiments followed the National Institutes of Health *Guide for the Care and Use of Laboratory Animals* under animal use protocols approved by the Chancellor's Animal Research Committee and Office for Animal Research Oversight at the University of California, Los Angeles, (UCLA) and at the University of California, Riverside (ARC #2007-035 and ARC #2019-0036, respectively). Experiments in Figure 1 used male and female FVB.129P2 WT mice (strain #004828, The Jackson Laboratory) and *Fmr1*$^{-/-}$ mice (Dutch-Belgian Fragile X Consortium, 1994; strain #004624, The Jackson Laboratory), and experiments in Figures 2-6 used male and female VIP-Cre mice (strain #010908, The Jackson Laboratory) that were crossed to the Ai9 (td-Tomato) reporter line (strain #007909, The Jackson Laboratory), and the resulting VIP-Cre x Ai9 mice were back crossed to FVB WT and *Fmr1*$^{-/-}$ mice for eight generations. All mice were housed in a vivarium with a 12/12 h light/dark cycle, and experiments were performed during the light cycle. The FVB background was chosen because of its robust breeding, because FVB *Fmr1*$^{-/-}$ dams are less prone to cannibalizing their pups, and because FVB *Fmr1*$^{-/-}$ mice have well-documented deficits in sensory processing (Contractor et al., 2015). We used separate homozygous litters of WT and *Fmr1*$^{-/-}$ mice rather than littermate controls because littermates of different genotypes tend to receive unequal attention from the dam (Zupan and Toth, 2008), which may affect the health and behavior of *Fmr1*$^{-/-}$ pups, biasing results. To avoid issues with genetic drift, we obtained new WT and *Fmr1*$^{-/-}$ breeders from The Jackson Laboratory at regular intervals (every 1–1.5 years).

Go/no-go visual discrimination task for head-restrained mice

A go/no-go visual discrimination task similar to that outlined in our prior study (Goel et al., 2018) was administered to awake, head-restrained young adult mice (beginning at 6–8 weeks) able to run on an air-suspended polystyrene ball treadmill. Beginning 5–7 d of recovery from head bar attachment and/or cranial window surgery, mice went through handling, habituation, and pretrials. Mice were handled gently for 5 min each day for 3 d until they were comfortable with the experimenter and would willingly transfer from one hand to the other. This was followed by water restriction, during which mice were given a rationed daily supply of water according to their weight and the habituation phase. During habituation, mice were acclimated to the behavior rig (and microscope for mice that were imaged) for 15 min each day. They were first head restrained and placed on the polystyrene ball and then gradually introduced to the visual stimuli, the lickport, the red light illuminating the ball, various sounds (fans circulating air in the rig, vacuum pump for water reward, scan mirrors), and objective for imaging. We started water restriction a few days before pretrials to motivate the mice to lick during pretrials (Guo et al., 2014). After habituation and achieving ~15–20% weight loss, mice were advanced to the pretrial phase.

During pretrials, sinusoidal gratings drifting in eight different directions (temporal frequency of 2 Hz, spatial frequency of 0.01 cycles/degree, and 100% contrast) were displayed on the monitor screen (23 inch display; Dell P2311HB or ThinkVision T24i-10). The monitor was placed 25 cm away from the mouse, and stimuli were presented at random for 3 s, with a 3 s intertrial interval (ITI) in which a gray screen was presented. Each stimulus was initially coupled with a small water reward (~3 μL) dispensed from the lickport beginning 2 s after the onset of stimulus presentation and up until the 3 s time point when the stimulus ended (water reward window). Licking by the mouse interrupted an infrared beam within the lickport (custom built at the UCLA electronics shop), which triggered a solenoid valve for water delivery, all of which was controlled via a data acquisition board (USB X Series Multifunction DAQ USB-6343, National Instruments). The mice were required to learn to associate this water reward with the presentation of the stimulus and lick during the water reward window. If an animal was not licking during the initial days of pretrials, the experimenter would pipette tiny drops of water onto the lickport every 30 trials to coax the animal to lick. Once mice had achieved a 80–85% licking rate, they were advanced to the visual discrimination task. We found no significant difference in the number of pretrial sessions it took to achieve this licking threshold between WT and *Fmr1*$^{-/-}$ mice (WT, 3.7 ± 0.4 sessions vs *Fmr1*$^{-/-}$, 3.2 ± 0.3 sessions; $p = 0.195$, unpaired, Student's t test).

During the go/no-go visual discrimination task, sinusoidal gratings drifting at two different directions (orthogonal orientations) were randomly presented on the screen for 3 s. The water reward was only delivered for the preferred stimulus (45° orientation), beginning 2 s after stimulus onset but not for the nonpreferred stimulus (135° orientation; Fig. 1*A*). Mice had to learn to discriminate between the two stimuli and to lick in anticipation of the water reward for the preferred stimulus (go trial) while withholding licking for the nonpreferred stimulus (no-go trial). Licking was recorded during the entire 3 s period, although only licking occurring in the reward window was rewarded. Depending on

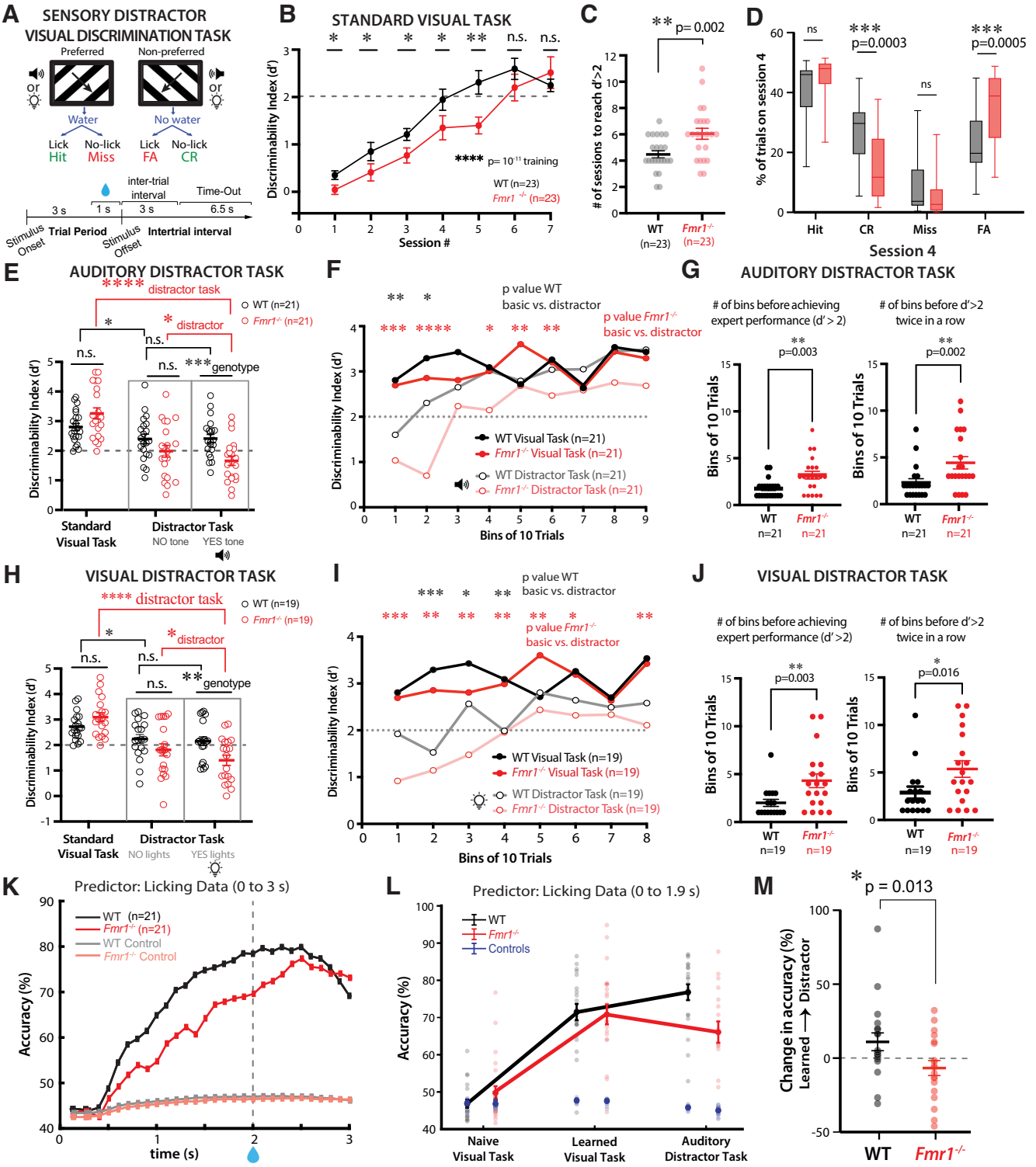

Figure 1. *Fmr1*$^{-/-}$ mice exhibit a decline in performance on the visual discrimination task in the presence of sensory distractors. ***A***, Illustration and timeline of behavior paradigm for visual discrimination task with auditory or visual distractors (90° difference between preferred and nonpreferred stimuli). Auditory or visual distractors were presented on 50% of trials coinciding with visual stimuli. CR, Correct Rejection; FA, False Alarm. ***B***, *Fmr1*$^{-/-}$ mice exhibited delayed learning of the basic visual task (Friedman test with repeated measures for training effect, followed by Mann–Whitney test for genotype effect at each session, $F_{(4,46)} = 70.15$, $p = 10^{-11}$; session 1, $p = 0.05$; session 2, $p = 0.025$; session 3, $p = 0.032$; session 4, $p = 0.05$; session 5, $p = 0.007$; session 6, $p = 0.443$; session 7, $p = 0.953$). Performance is measured by the discriminability index (d'). The dashed line at $d' = 2$ indicates expert performance threshold. WT mice consisted of 8 females and 15 males; *Fmr1*$^{-/-}$ mice consisted of 8 females and 15 males. ***C***, *Fmr1*$^{-/-}$ mice took longer to achieve $d' > 2$ (4.5 ± 0.3 sessions for WT mice vs 6.0 ± 0.4 sessions for *Fmr1*$^{-/-}$ mice; Mann–Whitney test, $p = 0.002$). ***D***, *Fmr1*$^{-/-}$ mice obtained a significantly lower percentage of CR responses (27.5 ± 2.2% for WT mice vs 14.6 ± 2.3% for *Fmr1*$^{-/-}$ mice; Mann–Whitney test, $p = 0.0003$) and a significantly higher percentage of FA responses (22.5 ± 2.2% for WT mice vs 35.3 ± 2.4% for *Fmr1*$^{-/-}$ mice; Mann– Whitney test, $p = 0.0005$) on session 4 of the visual task. There was no significant difference between genotypes in percentage of hit responses (41.6 ± 2.0% for WT mice vs 45.4 ± 1.3% for *Fmr1*$^{-/-}$ mice; Mann–Whitney test, $p = 0.103$) or percentage of miss responses (8.4 ± 2.0% for WT mice vs 4.7 ± 1.3% for *Fmr1*$^{-/-}$ mice; Mann–Whitney test, $p = 0.076$). ***E***, The performance of WT and *Fmr1*$^{-/-}$ mice was indistinguishable once they surpassed the expert threshold of $d' = 2$ (2.8 ± 0.1 for WT mice vs 3.3 ± 0.2 for *Fmr1*$^{-/-}$ mice; Mann–Whitney test, $p = 0.101$). During the distractor session, there were no genotype differences in d' on trials without distractors (2.4 ± 0.2 for WT mice vs 2.0 ± 0.2 for *Fmr1*$^{-/-}$ mice; Mann–Whitney test, $p = 0.109$). During trials with

the stimulus presented, the behavioral response (licking or the lack thereof) was recorded as a Hit, Miss, Correct Rejection (CR), or False Alarm (FA; Fig. 1*A*). An incorrect response (a Miss during a preferred trial or an FA on a nonpreferred trial) resulted in a time-out period (an extension of the ITI gray screen) of 6.5 s, during which the animal had to wait until the next trial. On session 6 of training, if mice had not improved in performance or reached a d' of at least 1, the punish time was either decreased to 4.5 s if there were too many misses or increased to 9.5 s if there were too many FAs. Each training session consisted of 350 trials, and only the last 100 trials were used to calculate the daily performance as the d' statistic or discriminability index as follows:

$$\mathrm{d'(dprime)} = \mathrm{norminv(fraction\ of\ Hits)}–\mathrm{norminv(fraction\ of\ FAs)}.$$

Norminv is a MATLAB function that returns the inverse of the normal cumulative distribution function. Custom written MATLAB scripts and Psychtoolbox were used to deliver the visual stimuli, dispense water from the lickport, and acquire data.

Distractor task for head-restrained mice

Once mice had maintained a $d' > 2$ (the threshold we chose for expert performance) for two consecutive sessions (i.e., stable performance), they were advanced to the distractor task, during which auditory or visual sensory distractors were delivered in the beginning of stimulus presentation. The auditory distractor consisted of one beep at 5 kHz and ~65 dB, lasting for 1.5 s and delivered from two speakers situated on either side of the monitor. For the visual distractor, we used LED lights (custom made at UCLA; 580–590 nm) wrapped around the monitor (flashing 4× for 0.5 s each with a 0.25 s interstimulus interval). Distracting stimuli were delivered in only ~50% of the trials at random, and each session consisted of 200 trials. Mice performed one session of the distractor task with auditory distractors and one session of the distractor task with visual distractors on successive days; the order of the modality of the distractor task was randomized. After the distractor task, another session was conducted using the standard visual discrimination task without distractors. Finally, a control session was conducted at the very end, where mice performed the task without any visual stimuli displayed on screen to ensure that performance was dependent on stimulus presence. For two-photon calcium imaging, a subset of mice was imaged at various time points of the training, initially before training (baseline recordings of visually evoked activity without behavior) and during the distractor task.

Human participants

Nineteen males with FXS and 20 male typically developing healthy controls (TDCs), matched on chronological age, completed the visual discrimination experiment (Extended Data Table 2–1). Four FXS and two TDC females also performed the experiment. Testing was conducted at a regional academic pediatric medical center where the participants with FXS were originally recruited as part of our Center for Collaborative Research in Fragile X Specialized center cooperative grant (U54HD104461). Approval for this study was granted through the Institutional Review Board at Cincinnati Children's Hospital Medical Center. All participants or their legal guardians, when appropriate, provided informed written consent and/or assent before participating. Diagnosis of FXS was confirmed via Southern blot and PCR assays performed at Rush University in the laboratory of Elizabeth Berry-Kravis. Seven males with mosaicism (size and/or methylation) were included in all analyses unless otherwise noted. No participants had a history of nonfebrile seizures or treatment with an anticonvulsant medication. Control participants were recruited through hospital-wide and community advertisements and were excluded for a history of

←

auditory distractors, *Fmr1*$^{-/-}$ mice performed significantly worse (2.4 ± 0.1 for WT mice vs 1.7 ± 0.2 for *Fmr1*$^{-/-}$ mice; Mann–Whitney test, $p = 0.001$). There was no difference between trials without distractors and trials with distractors for WT mice (2.4 ± 0.2 for no-distractor trials vs 2.4 ± 0.1 for distractor trials; Wilcoxon matched-pairs signed rank test, $p = 0.973$), whereas *Fmr1*$^{-/-}$ mice performed significantly worse on distractor trials (2.0 ± 0.2 for no tone trials vs 1.7 ± 0.2 for yes tone trials; Wilcoxon matched-pairs signed rank test, $p = 0.024$). For WT mice, performance on the distractor trials was slightly worse than performance during the standard visual task (2.8 ± 0.1 for visual task vs 2.4 ± 0.1 for distractor trials; Wilcoxon matched-pairs signed rank test, $p = 0.01$). However, there was a more significant decline in performance of *Fmr1*$^{-/-}$ mice (3.3 ± 0.2 for visual task vs 1.4 ± 0.2 for distractor trials; Wilcoxon matched-pairs signed rank test, $p = 9.5E\text{-}7$). For the auditory distractor task, WT mice consisted of 7 females and 14 males; *Fmr1*$^{-/-}$ mice consisted of 7 females and 14 males. ***F***, Performance (d') tracked throughout the auditory distractor task (trials grouped into bins of 10). *Fmr1*$^{-/-}$ mice took longer to recover to expert level than WT controls and never reached prior levels of performance (two-way mixed ANOVA for WT basic vs distractor; time, $F_{(7,269)} = 4.4$, $p = 8.6E\text{-}5$; task type, $F_{(1,40)} = 0.8$, $p = 0.377$; two-way mixed ANOVA for *Fmr1*$^{-/-}$ basic vs distractor; time $F_{(7,260)} = 5.1$, $p = 1.3E\text{-}5$; task type, $F_{(1.39)} = 11.5$, $p = 0.002$; time × task type, $F_{(12,421} = 1.9$, $p = 0.033$; two-way mixed ANOVA for WT learned vs *Fmr1*–/– learned; time, $F_{(8,321)} = 2.5$, $p = 0.011$; genotype, $F_{(1,40)} = 0.02$, $p = 0.883$; time × genotype, $F_{(12,479)} = 1.3$, $p = 0.217$; two-way mixed ANOVA for WT distractor vs *Fmr1*$^{-/-}$ distractor; time, $F_{(6,203)} = 8.9$, $p = 6.1E\text{-}9$; genotype, $F_{(1,39)} = 14$, $p = 5.9E\text{-}4$). ***G***, Performance throughout the auditory distractor task, the number of bins of trials before mice achieved expert performance ($d' > 2$) and before they got a $d' > 2$ twice consecutively was recorded. *Fmr1*$^{-/-}$ mice took longer before reaching a $d' > 2$ on a single bin (1.8 ± 0.2 for WT mice vs 3.2 ± 0.4 for *Fmr1*$^{-/-}$ mice; Mann–Whitney test, $p = 0.003$, $n = 21$ WT mice and 21 *Fmr1*$^{-/-}$ mice) and longer before getting a $d' > 2$ twice in a row than WT mice took (2.3 ± 0.4 for WT mice vs 4.4 ± 0.7 for *Fmr1*$^{-/-}$ mice; Mann–Whitney test, $p = 0.002$, $n = 21$ WT mice and 21 *Fmr1*$^{-/-}$ mice). ***H***, There was no significant difference between performance (measured by the discriminability index) of WT and *Fmr1*$^{-/-}$ mice once they reached the expert performance threshold of $d' = 2$ on the standard visual task (2.8 ± 0.1 for WT mice vs 3.1 ± 0.2 for *Fmr1*$^{-/-}$ mice; Mann–Whitney test, $p = 0.125$, $n = 19$ WT mice and 19 *Fmr1*$^{-/-}$ mice). On distractor sessions, during trials without distractors, there was no significant difference between performance of WT and *Fmr1*$^{-/-}$ mice (2.2 ± 0.2 for WT mice vs 1.8 ± 0.2 for *Fmr1*$^{-/-}$ mice; Mann–Whitney test, $p = 0.163$). During trials with visual distractors, *Fmr1*$^{-/-}$ mice exhibited worse performance than WT mice (2.1 ± 0.2 for WT mice vs 1.4 ± 0.2 for *Fmr1*$^{-/-}$ mice; Mann–Whitney test, $p = 0.0097$). There was no significant difference between WT performance on trials without distractors versus trials with distractors on the visual distractor session (1.8 ± 0.2 for no light trials vs 1.4 ± 0.2 for yes light trials; Wilcoxon matched-pairs signed rank test, $p = 0.829$). However, *Fmr1*$^{-/-}$ mice exhibited worse performance on trials with distractors than on trials without distractors (2 ± 0.2 for no light trials vs 1.7 ± 0.2 for yes light trials; Wilcoxon matched-pairs signed rank test, $p = 0.032$). For WT mice, performance on the distractor trials was slightly worse than performance during the standard visual task (2.8 ± 0.1 for visual task vs 2.1 ± 0.2 for distractor trials; Wilcoxon matched-pairs signed rank test, $p = 0.011$). However, the decline in performance of *Fmr1*$^{-/-}$ mice was more severe (3.3 ± 0.2 for visual task vs 1.7 ± 0.2 for distractor trials; Wilcoxon matched-pairs signed rank test, $p = 3.8E\text{-}6$). WT mice consisted of 7 females and 12 males; *Fmr1*$^{-/-}$ mice consisted of 7 females and 12 males. ***I***, *Fmr1*$^{-/-}$ mice were more sensitive to distracting lights than WT mice. Performance (d') was tracked throughout the last session of the visual discrimination task when learning has occurred and compared with performance throughout distractor trials on the distractor session; trials were grouped into bins of 10 trials. *Fmr1*$^{-/-}$ performance took longer to recover to expert level and continued to be significantly worse than prior levels of performance throughout the duration of the task (two-way mixed ANOVA for WT basic vs distractor, time, $F_{(8,257)} = 1.4$, $p = 0.07$; task type, $F_{(1,36)} = 10$, $p = 0.003$; two-way mixed ANOVA for *Fmr1*$^{-/-}$ basic vs distractor, time, $F_{(7,243)} = 3.4$, $p = 0.002$; task type, $F_{(1,39)} = 18.1$, $p = 1.3E\text{-}4$; two-way mixed ANOVA for WT learned vs *Fmr1*$^{-/-}$ learned; time, $F_{(8,360)} = 2.7$, $p = 0.006$; genotype, $F_{(1,44)} = 0.3$, $p = 0.594$; time × genotype, $F_{(12,526)} = 1.2$, $p = 0.298$; two-way mixed ANOVA for WT distractor vs *Fmr1*$^{-/-}$ distractor; time, $F_{(6,164)} = 3.6$, $p = 0.002$; genotype, $F_{(1,31)} = 2.4$, $p = 0.013$). ***J***, Performance throughout the visual distractor task. *Fmr1*$^{-/-}$ mice took longer before reaching a $d' > 2$ on a single bin (2 ± 0.4 for WT mice vs 4.3 ± 0.7 for *Fmr1*$^{-/-}$ mice; Mann–Whitney test, $p = 0.003$; $n = 17$ WT mice and 19 *Fmr1*$^{-/-}$ mice) and longer before getting a $d' > 2$ twice in a row than WT mice took (2.9 ± 0.6 for WT mice vs 5.4 ± 0.8 for *Fmr1*$^{-/-}$ mice; Mann–Whitney test, $p = 0.016$, $n = 17$ WT mice and 19 *Fmr1*$^{-/-}$ mice). ***K***, SVM classifier from lick data predicts stimulus type with greater accuracy in WT mice than *Fmr1*$^{-/-}$ mice. Averages of 10,000 iterations for each mouse for each 0.1 s bin of time during the 3 s stimulus period. For controls, stimuli were randomly shuffled. ***L***, Accuracy of SVM classifier at different stages of task. Symbols represent individual mice. Controls (shuffled stimuli) are shown in blue. ***M***, Change in accuracy of predicting stimulus type based on licking data from the learned session to the auditory distractor task (***E***), was significantly different between genotypes (+11.1 ± 6.0% for WT mice vs −6.7. ± 5.1% for *Fmr1*$^{-/-}$ mice; Mann–Whitney test, $p = 0.013$). Horizontal bars (***B–M***) indicate mean, and error bars indicate SEM; *n* values are for mice, indicated on each plot; *$p < 0.05$, **$p < 0.01$, ***$p < 0.001$, ****$p < 0.0001$.

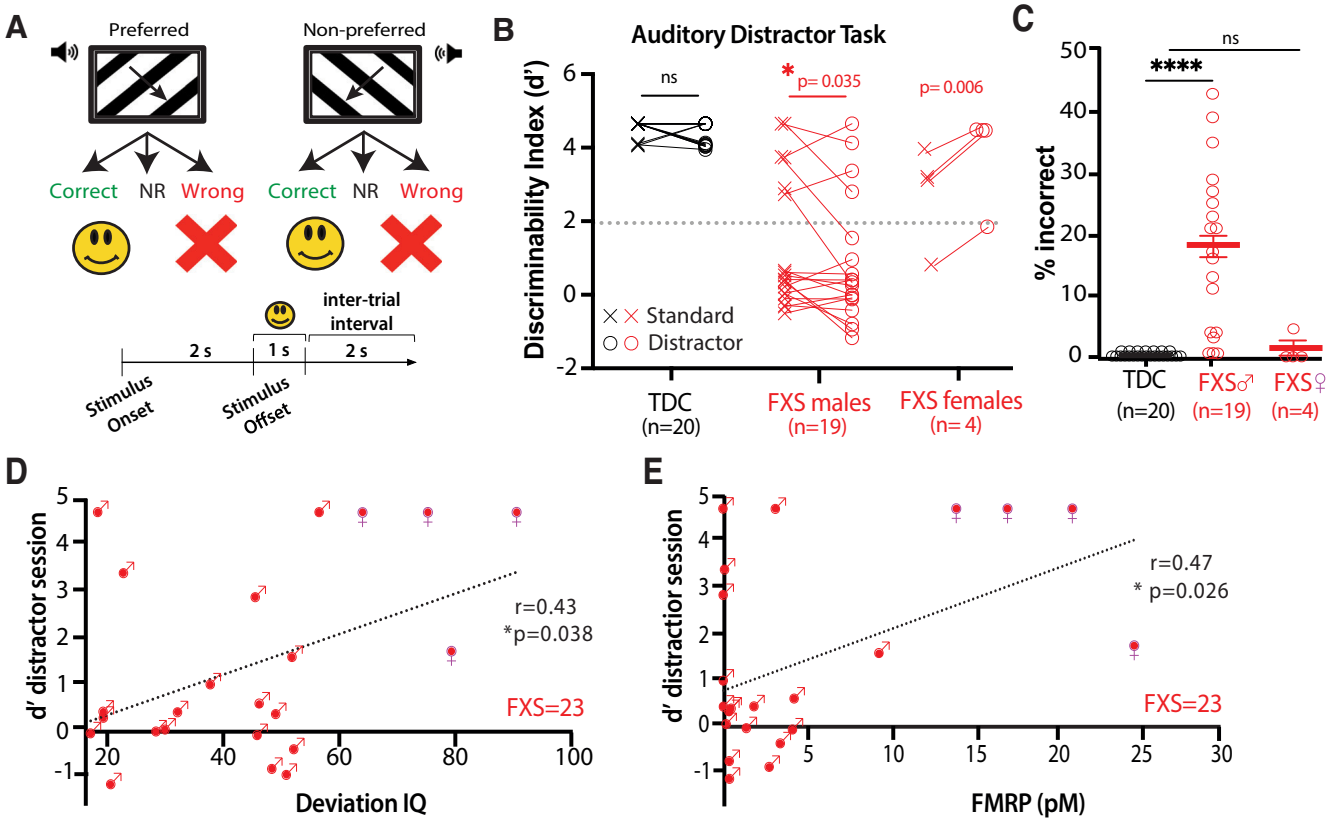

Figure 2. Males with FXS exhibit a significant decline in visual discrimination with auditory distractors. ***A***, Illustration and timeline of behavior paradigm for auditory distractor visual discrimination task in humans. Auditory distractors consisted of tones and were presented on 50% of trials. ***B***, Compared with TDCs, FXS male participants (middle column) showed a significant decrease in d' in the presence of distractors, FXS females (right column) exhibited a higher d' on the distractor session (TDC males, Standard task $d' = 4.6 \pm 0.2$; Distractor task $d' = 4.4 \pm 0.3$; $p = 0.07$; FXS males, Standard task $d' = 1.3 \pm 0.4$; Distractor task $d' = 0.8 \pm 0.4$; $p = 0.03$, paired t test; FXS females, Standard task $d' = 2.6 \pm 0.7$; Distractor task $d' = 3.9 \pm 0.7$; $p = 0.006$, paired t test). ***C***, FXS male participants showed a higher percentage of incorrect responses on the distractor task ($0.3 \pm 0.1\%$ in TDC vs $17.4 \pm 3.1\%$ in FXS; t test, $p = 4.0E\text{-}5$). Incorrect responses from FXS female participants were not significantly different from TDC. Horizontal bars indicate mean ± SEM. ***D***, Higher deviation IQ related to better performance in presence of the auditory distractor ($r = 0.43$, $p = 0.038$). This relationship was not significant when performed with males only. ***E***, Increased FMRP expression related to better performance with distractors ($r = 0.47$, $p = 0.026$). This relationship was not significant when performed with males only. Extended Data Table 2–1 shows demographic information of the individuals tested.

developmental or learning disorders or significant psychiatric disorder (e.g., schizophrenia) in themselves or first-degree relatives or for a family history of autism spectrum disorder (ASD) in first- or second-degree relatives based on a brief screening interview. All study procedures were approved by the local institutional review board.

Visual discrimination and distractor task for human participants

Human FXS and control participants completed a visual discrimination task, followed by a distractor task that was analogous to that used with mice, with relatively minor modifications. Because of the additional cognitive demands of a go/no-go paradigm, including inhibitory control, which is known to be impaired in FXS (Hooper et al., 2008), we designed a forced two-choice visual discrimination task so that all FXS participants could learn and perform the task. Although it is possible that participants with FXS could have learned the go/no-go task with subsequent training sessions, just as the mice required consecutive sessions to learn, because of time constraints and a significant burden on the patient population, this limited our ability to do so. Visual gratings were displayed via Psychtoolbox using MATLAB software version 2016a on a 23 inch Tobii TX300 monitor and responses were made on designated keys on the keyboard. During the task, when the visual grating appeared to move from the right side to left side, subjects were instructed to press the corresponding left-sided key (Z), and when the visual grating appeared to move from left to right, subjects were instructed to press the corresponding right-sided key (M). If participants correctly responded to the direction of the stimulus, they received positive visual feedback (e.g., image of a popular video game cartoon character). If participants incorrectly responded to the direction of the stimulus, they received negative visual feedback (e.g., a large red X). If no response was received, no feedback was given. Visual gratings appeared on screen for up to 2 s or until participant response, at which point immediate feedback was presented for 1 s. Although the stimulus disappeared at 2 s, participants had until 3 s poststimulus onset to respond and receive valid feedback. There was an intertrial interval of 2 s. All participants completed the first-order discrimination task, immediately followed by the distractor task in which auditory distractors were presented simultaneously with the visual stimuli for 50% of the trials at random.

Before administration of the initial task, participants received verbal instructions and then verified initial task comprehension by verbally and/or nonverbally demonstrating their expected behavioral response (i.e., pointing to left). Next, participants completed at least one block of 15 trials, in which vertical lines moved from left to right on the screen (or right to left), and participants were instructed to press the corresponding key based on the direction the lines moved. All participants included in the sample met practice criterion. Depending on the stimulus presented, the subject's behavioral response was characterized as Right (similar to Hit), No response (NR), or Wrong (similar to FA). As this was a forced two-choice visual discrimination task, a modified d prime, or d' (discriminability index), was calculated as follows:

$$dprime = Norminv\,(fraction\ of\ Rights) – norminv\,(fraction\ of\ Wrongs).$$

Additional measures for human participants

All participants completed the abbreviated *Stanford–Binet Intelligence Scales, Fifth Edition* (SB5) to estimate general intellectual functioning. Based on previous studies (Sansone et al., 2014), we converted standard

scores to Deviation IQ scores to reduce floor effects present for individuals with severe cognitive impairments and to better evaluate interindividual variability.

In addition, we collected caregiver report measures of behavior and psychiatric symptoms, including hyperactivity (Aberrant Behavior Checklist; Aman et al., 1985); from the Anxiety, Depression, and Mood Scale (Esbensen et al., 2003); as well as sensory sensitivity (Brown and Dunn, 2002) to relate to task performance. Participants with FXS also completed a computerized Kiddie Test of Attentional Performance (KiTAP), which has been validated for use in this population (Knox et al., 2012). KiTAP examines executive functioning through multiple subtests, including Alertness (processing speed), Distractibility (attention), Go/NoGo (response inhibition), and Flexibility (cognitive flexibility). The number of correct trials on tasks were examined in relation to correct trials on the visual discrimination task with distractors. Eleven participants did not complete KiTAP because of behavior issues and/or time constraints.

Last, whole-blood samples were obtained via venipuncture from participants with FXS and analyzed using our validated Luminex-based immunoassay to determine levels of FMRP (fragile x messenger ribonucleoprotein; Boggs et al., 2022). Briefly, blood samples were spotted onto Whatman Bloodstain cards, and then dried blood spots were hole punched from the cards, and proteins were eluted. The eluate was analyzed in triplicate against a nine-point standard curve generated from a recombinant protein to determine participants' FMRP concentration. One participant with FXS did not consent to blood draw.

Support Vector Machine

To analyze the licking data, we used the Support Vector Machine (SVM) available in the MATLAB Machine Learning and Deep Learning toolbox via the function *fitcsvm*. SVMs are supervised learning models with learning algorithms that can be used to classify data in a high-dimensional space; it uses a subset of training points to develop a binary classifier that can use features of the data to make predictions. We used a radial basis function as the kernel. Eighty percent of our data was applied to training the machine and 20% applied to testing it.

We performed two types of analysis using the SVM. We first binned licking into 0.1 s bins. We then used the bins before the water reward (0–1.9 s) as the feature space of the SVM and then performed a bootstrap of 1000 iterations in which licking was the predictor of stimulus type per mouse per session day. This generated a distribution of accuracy percentages that were then averaged. Additionally, to determine the most predictive features, we performed a bootstrapped SVM per feature of 10,000 iterations to determine the most predictive features per mouse per session day (e.g.., the predictability of licking at the 0.1 s bin in the naive day). This again provided a distribution of accuracy percentages that were then averaged and plotted as a function of time. For each SVM set, we performed controls in which stimuli were randomly shuffled.

Viral constructs

Both pGP-AAV-syn-jGCaMP7f-WPRE and pGP-AAV-syn-FLEX-jGCaMP7f-WPRE were purchased from Addgene (catalog #104488-AAV1 and catalog #104492-AAV1) and diluted to a working titer of 1×10^{13} (to enable a longer period of optimal expression) with 1% filtered Fast Green FCF dye (Thermo Fisher Scientific). We injected (see below) a cocktail of these viruses to improve the efficacy of viral expression in pyramidal and VIP cells.

Cranial window surgery

Craniotomies were performed at 6–8 weeks as previously described (Mostany and Portera-Cailliau, 2008; Holtmaat et al., 2009). Briefly, mice were anesthetized with isoflurane (5%, 1.5–2% maintenance), head fixed to a stereotaxic frame, and, under sterile conditions, a 4.5-mm-diameter craniotomy was drilled over the V1 and covered with a 5 mm glass coverslip using cyanoacrylate glue and dental cement. Before placing the coverslip, we injected ~60–100 nL of a cocktail of pGP-AAV-syn-jGCaMP7f-WPRE and pGP-AAV-syn-FLEX-jGCaMP7f-WPRE using a programmable nanoliter Injector (Nanoject III, Drummond Scientific). A U-shaped titanium bar was attached to the skull with dental cement to head restrain the animal during behavior and calcium imaging. For a subset of mice that underwent behavioral testing but no calcium imaging, only a head bar attachment surgery was performed (no craniotomy). All mice were administered dexamethasone (0.2 mg/kg) intraperitoneally or subcutaneously on the day of surgery to prevent swelling of the brain; a subset of mice was also administered carprofen (5 mg/kg) as an analgesic and anti-inflammatory). After surgery, mice were placed on a heated pad for postoperative recovery until effects of the anesthesia wore off. Postoperative checks were done every 24 h for the following 2 d to ensure a healthy, full recovery.

In vivo two-photon calcium imaging

Two-photon calcium imaging was performed on a Scientifica two-photon microscope equipped with a Chameleon Ultra II Ti:sapphire laser (Coherent) tuned to 920–940 nm, resonant scanning mirrors (Cambridge Technologies), a 20× objective (1.05 NA, Olympus), multi-alkali photomultiplier tubes (R3896, Hamamatsu) and ScanImage software (Pologruto et al., 2003). Before calcium imaging, head-restrained mice were habituated to a soundproof chamber and allowed to run freely on a polystyrene ball and acclimated to the rig as described above for the visual task. To record visually evoked activity, we presented visual stimuli consisting of full-field sinusoidal drifting gratings (16 random repeats of 8 orientations) presented for 3 s each and separated by a 3-s-long gray screen interstimulus interval. Both spontaneous and visually evoked responses of L2/3 pyramidal cells and VIP cells from V1 were recorded at 15 Hz in two to four fields of view. In Figure 3, each FOV consisted of a median of 64 pyramidal cells (range was 62–91 for WT and 30–108 cells for *Fmr1*$^{-/-}$ mice). In Figure 4, each FOV consisted of a median of four VIP cells (range was 1–10 cells for WT and 2–10 cells for *Fmr1*$^{-/-}$ mice). In Figures 5 and 6, each FOV consisted of a median of six VIP cells (range was 4–12 cells for WT and 4–13 cells for *Fmr1*$^{-/-}$ mice). In each animal, imaging was performed at a depth of 150–200 μm, and data were averaged from movies collected across all FOVs.

Data analysis for calcium imaging

All calcium imaging data were initially processed using Suite2p or EZcalcium software and algorithms (Pachitariu M et al., 2017; Cantu et al., 2020) for image registration, region of interest (ROI) detection, cell identification, and signal extraction with neuropil correction. This was done separately for pyramidal cells and VIP cells. Once Suite2p had performed a rigid and nonrigid registration and then detected ROIs using a classifier, we then selected cells after visual inspection of the shape of the ROI and its fluorescence trace for quality control purposes. Next, the extracted fluorescence signal intensities for each ROI (F) were processed with custom-written MATLAB routines, which included modifications of our previously described code (Goel et al., 2018). A modified Z-score, Z_f (t) vector representing the activity levels of each neuron, was calculated as follows:

$$Z_f(t) = \frac{F(t) - mean(baseline)}{std(baseline)},$$

where the baseline period is the 10 s quietest period with the lowest variation (SD) in $\Delta F/F$ (He et al., 2017). All subsequent analyses were performed using the Z_f (t) vectors.

Neuropil subtraction was performed by removing the local fluorescence signal surrounding each ROI (Chen et al., 2013; He et al., 2017; Pachitariu et al., 2017). Peaks of activity were then detected in the Z-scores using the peakfinder MATLAB script. These peaks were used to calculate the mean Z-score fluorescence (an estimate of amplitude of the fluorescence signal) and the frequency of events. To remove any bias resulting from peak detection, especially in VIP cells, we also calculated the frequency of events based on the magnitude of the fluorescence signal [area under the curve (AUC)]. For this analysis, we calculated the AUC for each fluorescence trace and divided that by the number of frames during which a stimulus occurred (i.e., 45 frames at 15 Hz for for 3 s). This was then multiplied by the frame rate to get a Z-score of fluorescence (mean activity) per second (Figs. 4–6).

To quantify visually evoked activity, we averaged the responses of neurons during the 3 s of visual stimulation and the 3 s of gray screen before the next stimulus. To quantify spontaneous activity, we conducted separate recordings during which the animals were presented a

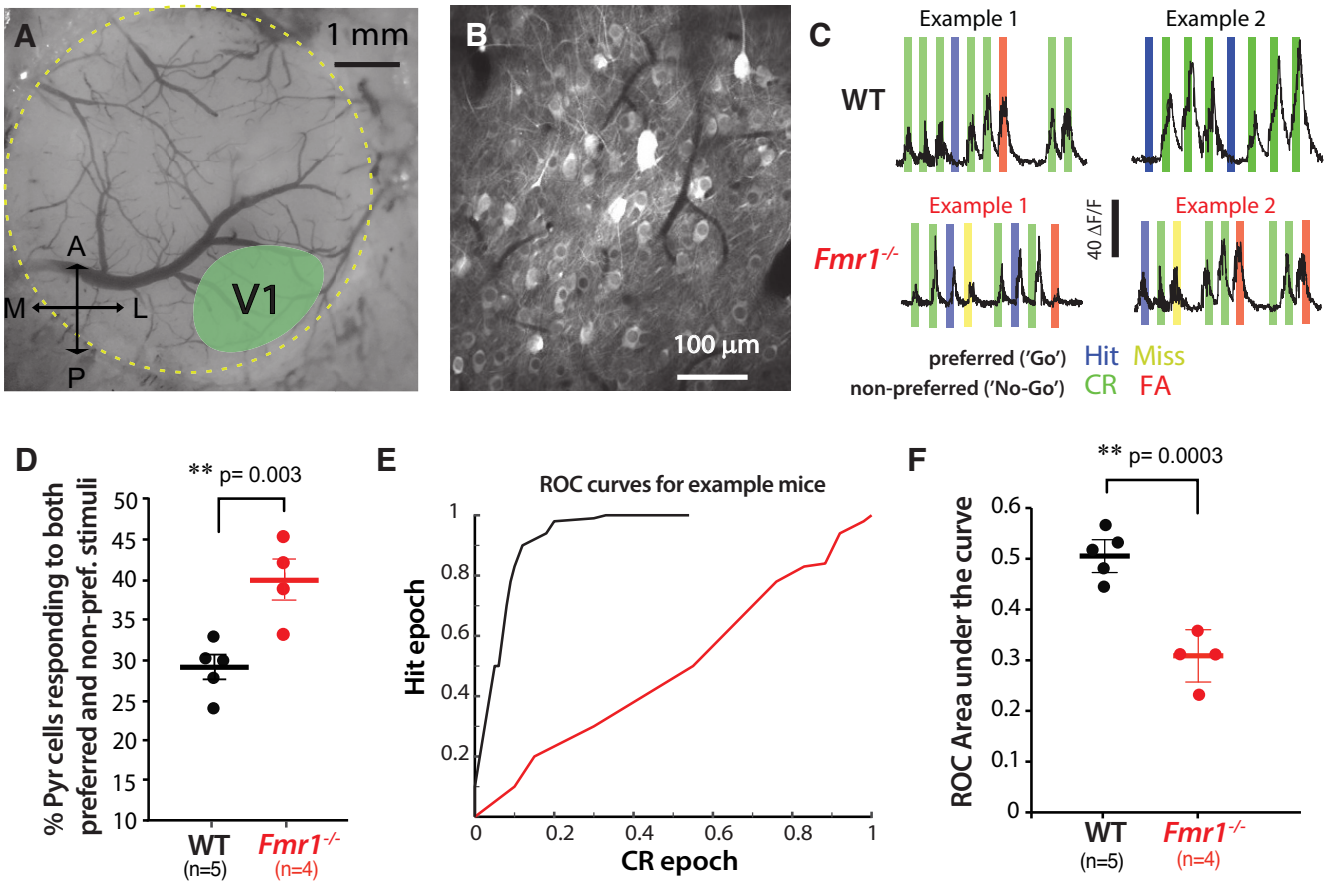

Figure 3. Reduced orientation selectivity of pyramidal cells after learning in *Fmr1*$^{-/-}$ mice. ***A***, Example cranial window showing approximate location of V1 (A, Anterior; P, posterior; M, medial; and L, lateral). ***B***, Representative field of view for *in vivo* two-photon calcium imaging of layer 2/3 pyramidal (Pyr) neurons in V1 expressing GCaMP7f. ***C***, Traces of visually evoked calcium transients for two example Pyr neurons during the distractor task from WT and *Fmr1*$^{-/-}$ mice. Responses (as determined by changes in jGCaMP7f fluorescence intensity, ΔF/F) were seen across both preferred and nonpreferred trials in *Fmr1*$^{-/-}$ mice, whereas Pyr neurons in WT mice were tuned to either or. ***D***, The percentage of Pyr cells that respond to both preferred and nonpreferred stimuli on the distractor task was higher in *Fmr1*$^{-/-}$ mice (28.7 ± 1.4% for WT mice vs 39.6 ± 2.6% for *Fmr1*$^{-/-}$ mice; *t* test, $p = 0.003$). ***E***, Example ROC curves (see above, Materials and Methods) for the data shown in example 2 in ***C***. ***F***, The mean area under the curve for the ROC was smaller in *Fmr1*$^{-/-}$ mice, consistent with the reduced selectivity of Pyr cells during the distractor task (0.5 ± 0.02 for WT mice vs 0.3 ± 0.03 for *Fmr1*$^{-/-}$ mice; *t* test, $p = 0.0003$).

static gray screen. To determine whether an individual cell was responsive to visual stimuli (Figs. 3, 4), we used a probabilistic bootstrapping method as described previously (He et al., 2017; Goel et al., 2018). First, we calculated the correlation between the stimulus time course and the Z_f vector, followed by correlation calculations between the stimulus time course and 1000 scrambles of all calcium activity epochs in Z_f (epoch = consecutive frames wherein $Z_f \geq 3$). The 1000 comparisons generated a distribution of correlations (r values), within which the correlation of the unscrambled data and the stimulus fell at any given percentile. If the calculated percentile for a cell was <1%, then we considered that cell as being stimulus selective.

The modulation index was calculated to compare changes in activity (Figs. 4–6). In Figure 4 we compared visually evoked activity of VIP cells with their spontaneous activity and measured the change in activity (i.e., the difference between gray screen and drifting gratings). In Figures 5 and 6, we compared VIP activity during correct responses (Hits and CRs) to activity during the majority of incorrect responses (FAs and Misses). We divided mean visually evoked activity during incorrect responses by mean visually evoked activity during correct responses to get the modulation index.

Receiver operating characteristic analysis

The discrimination performance of pyramidal neurons was quantified using a receiver operating characteristic (ROC) analysis (O'Connor et al., 2010). Neuronal output was classified based on the similarity of response on each trial to the mean poststimulus time histograms (PSTHs) for the Hit and CR trials. Mean PSTHs were computed separately for each hit trial and CR trial. For this calculation, the current trial was not included. Similar to O'Connor et al. (2010), each trial was then assigned a decision variable (DV) score, which was equal to the dot product similarity to the mean PSTH for Hit trials minus the dot product similarity to the mean PSTH for CR trails. Thus, DV was calculated using the following equations for Hit and CR trials, respectively:

$$DV = t\_i\,(\llbracket meanHit \rrbracket\_(k \neq i) - meanCR)$$

$$DV = t\_i\,(meanHit - \llbracket meanCR \rrbracket\_(k \neq i)),$$

where t_i is the PSTH for the current (ith trial) mean Hit and mean CR are the mean hit and CR PSTHs. In cases where the decision variable was large, it implied a higher similarity to the mean hit PSTH compared with the mean correct rejection PSTH. If the DV was greater than a criterion value, the trial was classified as Hit; otherwise, it was a correct rejection trial. To determine the proportion of correctly identified trials, an ROC curve was constructed (Green and Swets, 1966). The area under the ROC curve was calculated using the MATLAB function *trapz*.

Statistical analyses

In all figures, significance levels are indicated as follows: $^*p < 0.05$, $^{**}p < 0.01$, $^{***}p < 0.001$. The SEM is plotted using error bars unless otherwise noted. Graphs show either individual data points from each animal/human subject or group means (average over different mice or

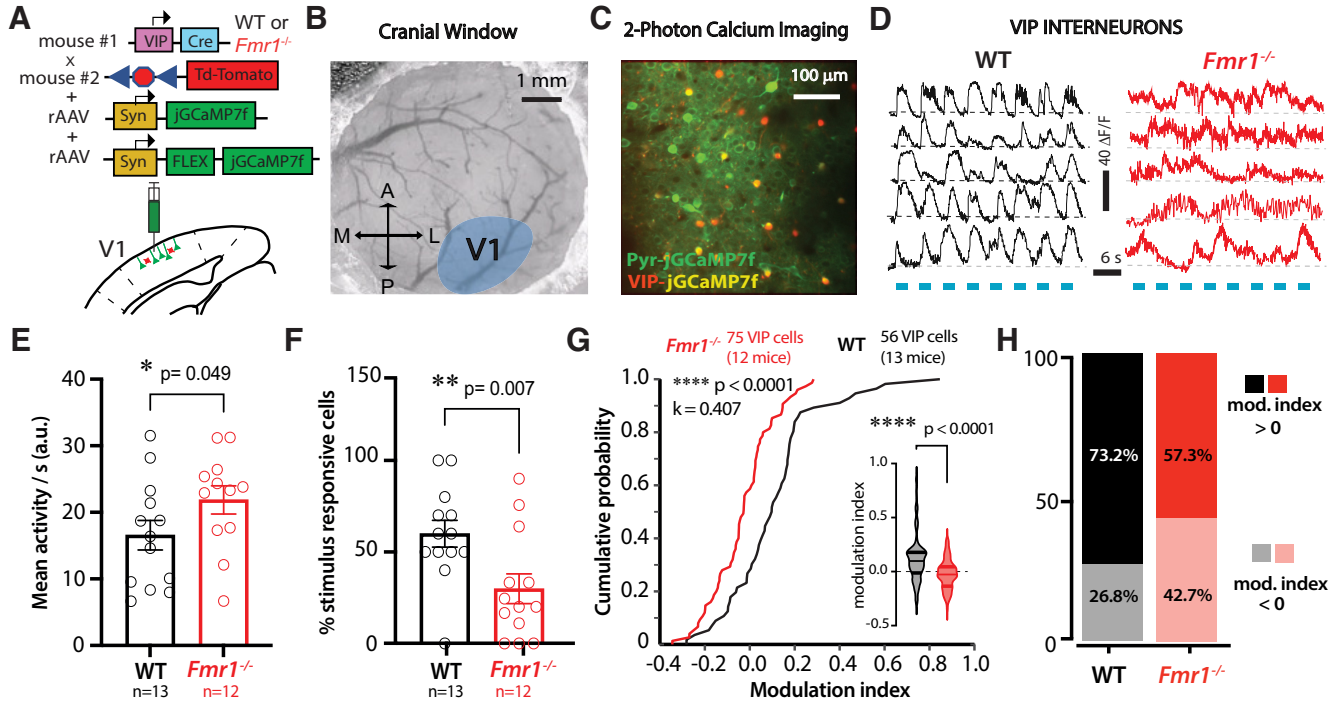

Figure 4. Reduced modulation by visual stimuli of VIP activity in *Fmr1*$^{-/-}$ mice. ***A***, Illustration of coinjection of rAAV-syn-jGCaMP7f and rAAV-syn-FLEX-jGCaMP7f in V1 in VIP-cre x ai9 mice (td-Tom). ***B***, Example cranial window over V1 (labels the same as in Fig. 3*A*). ***C***, Representative field of view for *in vivo* two-photon calcium imaging of Pyr (green) and VIP neurons (red-yellow). ***D***, Example traces of visually evoked calcium transients for VIP neurons in WT and *Fmr1*$^{-/-}$ mice. Blue bars represent epochs of sinusoidal gratings (drifting in 8 directions). ***E***, Mean visually evoked activity of VIP cells as measured by the area under the trace (a.u.) was higher in *Fmr1*$^{-/-}$ mice (16.6 ± 2.2 for WT mice vs 21.9 ± 2.1 for *Fmr1*$^{-/-}$ mice; Mann–Whitney test, $p = 0.049$, Cohen's $d = 0.691$). Symbols denote individual mice. ***F***, There were fewer VIP neurons in *Fmr1*$^{-/-}$ mice that were responsive to the visual stimuli (60 ± 7.3% for WT mice vs 29.9 ± 8.1% for *Fmr1*$^{-/-}$ mice; Mann–Whitney test, $p = 0.007$, Cohen's $d = 1.084$). ***G***, A cumulative probability plot showing reduced VIP cell modulation by visual stimuli for *Fmr1*$^{-/-}$ mice as measured by a modulation index (two-sample Kolmogorov–Smirnov test, $p = 2.81E\text{-}05$, $k = 0.407$). Violin plot inset shows reduced VIP modulation in *Fmr1*$^{-/-}$ mice; values indicate change in activity as a result of visual stimuli compared with gray screen (+0.11 ± 0.03 for WT mice vs −0.03 ± 0.02 for *Fmr1*$^{-/-}$ mice; Mann–Whitney test, $p = 8.44E\text{-}6$ Cohen's $d = 0.783$). ***H***, The percentage of VIP cells that were positively modulated by the visual stimuli was smaller in *Fmr1*$^{-/-}$ mice (57.3%) than in WT controls (73.2%).

human subjects) superimposed on individual data points. All statistical details are described in the figure legends, and tests were selected based on the distribution of the data points. For parametric two-group analyses, we used a Student's *t* test (paired or unpaired), and for multiple group analyses we used a one-way or two-way ANOVA. For nonparametric tests, we used the Mann–Whitney test, Welch's test, Friedman (repeated measures) test, and mixed-effects ANOVA (for datasets with missing values). Multiple comparisons were corrected and correlations were conducted using Pearson's *r*. For distributions, a two-sample Kolmogorov–Smirnov test was used. All statistical analyses were conducted using GraphPad Prism software or MATLAB.

Sample size

We determined sample sizes before experiments based on our past experience and the published literature and guided by ethical principles in the use of animals (i.e., trying to minimize the number of animals used). Based on our prior studies, we estimated that for behavioral studies a minimum of 15 animals per group would be needed, and for calcium imaging 5–6 mice would be needed. For results shown in Figure 1, we used sample sizes of ≥20 mice per genotype, whereas in Figure 3, we analyzed pyramidal cell data for a subset of mice ($n \geq 4$ for each group of mice). We used sample sizes of >10 for each group in Figure 4 and $n \geq 5$ mice per group in Figures 5 and 6. Subsequent statistics were performed using the number of mice or subjects as the sample size or the number of cells. We chose our sample sizes for feasibility and ethical purposes in our use of animals (i.e., trying to minimize the number of animals used).

Subsequent statistics were performed using the number of mice or subjects as the sample size or the number of cells. Given the low density of VIP cells, some of the analyses were done using cells as sample size, similar to other recent studies (Ren et al., 2022). However, the overall effects of reduced modulation of VIP cells on behavior was significant when mice were used as sample size (Fig. 5).

Randomization

We ensured that during each behavior training cycle both WT and *Fmr1*$^{-/-}$ mice were included to exclude any biases introduced by experimenters or the training rig. In addition, on a particular testing day, Fragile X participants were randomized with control subjects.

Blinding

Experimenters were blinded to the genotype while training mice on the task, and analysis was performed with experimenters blind to the genotype.

Neural data exclusion

We included only neurons that elicited at least one calcium transient during the duration of the recording; A small fraction of neurons was excluded because they were deemed inactive on the basis of calcium imaging data (percentage of pyramidal neurons excluded, WT = 0.1%; *Fmr1*$^{-/-}$ = 0.1%; VIP neurons excluded, WT = 0%, *Fmr1*$^{-/-}$ = 0.02%).

Exclusion of mice or human participants

Two mice were excluded from the dataset because they developed health conditions or died. And two additional mice were excluded from the dataset because the mice lost >25% of their original body weight, which could lead to less grooming, less social interaction with cage mates, lethargy, seizures, and other health conditions that might conflict with behavior.

Results

Fmr1$^{-/-}$ mice exhibit a delay in perceptual learning compared with WT controls

To investigate symptoms of ADD in FXS, we tested the effect of sensory distractors on decision-making using the same visual discrimination task with which we previously uncovered

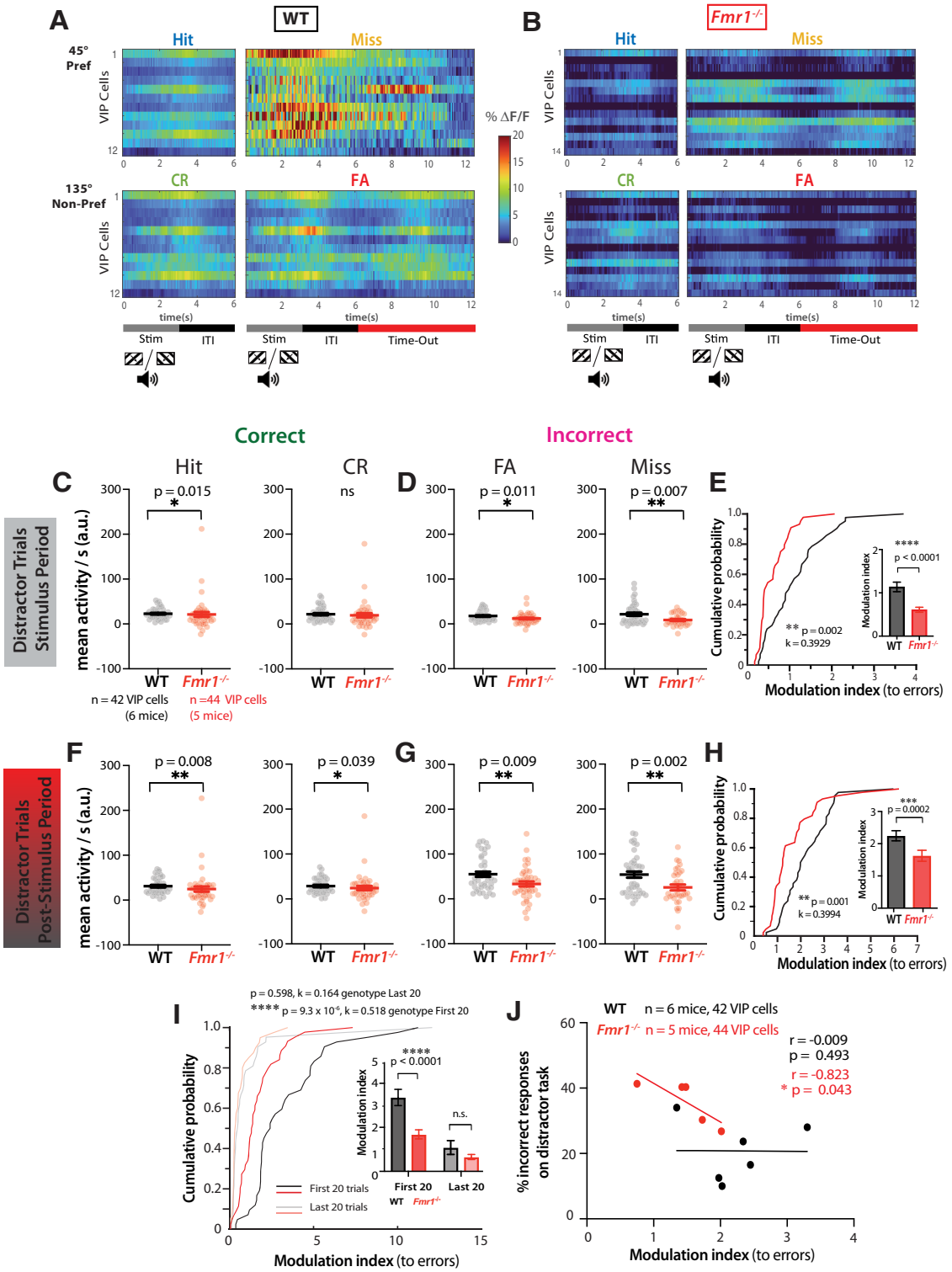

Figure 5. Reduced modulation of VIP activity by incorrect responses in *Fmr1*$^{-/-}$ mice correlates with delayed learning and poor performance on the distractor task. ***A***, Raster plots of individual VIP neuron activity in an example WT mouse sorted by trials of different response type—hits, misses, CRs, FAs. Two-photon calcium imaging was performed during the distractor task, and recordings were made from VIP neurons. Each row represents an average across all trials of the specific response type for that neuron. The timeline at the bottom denotes the visual stimulus presentation (0–3 s), the intertrial interval (3–6 s), and the time-out (6–12.5 s, only for misses and FAs). ***B***, Same as ***A*** but for VIP neurons from an example *Fmr1*$^{-/-}$ mouse. Note the lack of modulation of VIP cell activity during the stimulus period or the poststimulus (Stim) period. ***C***, Mean VIP activity during the stimulus period on auditory distractor trials (as measured by the area under the trace per second) was significantly lower in *Fmr1*$^{-/-}$ mice during hit trials (22.9 ± 1.9 for WT vs 21.2 ± 5.4 for *Fmr1*$^{-/-}$; Mann–Whitney test, $p = 0.015$, Cohen's $d = 0.064$). During CR trials, mean VIP activity was similar across genotypes (21.7 ± 2.4 for WT vs 19.3 ± 4.5 for *Fmr1*$^{-/-}$; Mann–Whitney test, $p = 0.072$). ***D***, Mean VIP activity was significantly lower in *Fmr1*$^{-/-}$ mice during FA trials (17.7 ± 1.8 for WT vs 12.0 ± 1.8 for *Fmr1*$^{-/-}$; Mann–Whitney test, $p = 0.011$, Cohen's $d = 0.482$) and during miss trials (21.8 ± 3.6 for WT vs 9.0 ± 2.2 for *Fmr1*$^{-/-}$; Mann–Whitney test, $p = 0.007$, Cohen's $d = 0.684$). ***E***, VIP cell modulation by incorrect responses (errors) was significantly lower in *Fmr1*$^{-/-}$ mice (two-sample Kolmogorov–Smirnov test, $p = 0.002$, $k = 0.3929$). Inset, Bar graph shows VIP cell modulation by errors (1.1 ± 0.7 for WT vs 0.6 ± 0.4 for *Fmr1*$^{-/-}$; Mann–Whitney test, $p =$ 2.0E-5, Cohen's $d =$ 0.916). ***F***, Mean VIP activity during the intertrial interval period on auditory distractor trials was significantly lower in *Fmr1*$^{-/-}$ mice during hit trials (31.0 ± 2.7 for WT vs 24.6 ± 5.7 for

converging perceptual learning deficits in both *Fmr1*$^{-/-}$ mice and humans with FXS (Goel et al., 2018). First, we trained awake, head-restrained, water-controlled young adult (2–3 months) male and female WT and *Fmr1*$^{-/-}$ mice ($n = 23$ for each genotype) on a go/no-go task in which mice had to discriminate between sinusoidal gratings drifting in two orthogonal directions (see above, Materials and Methods). Specifically, they had to learn to lick for a water reward for the preferred stimulus (45° orientation) but withhold licking for the nonpreferred stimulus (135° orientation; Fig. 1*A*). Correct behavioral responses included hits and CRs, whereas incorrect responses (errors) included misses and false alarms (FAs), both of which resulted in a time-out punishment period of 6.5 s. Task performance was determined by the discriminability index statistic d' (see above, Materials and Methods). As we previously reported (Goel et al., 2018), *Fmr1*$^{-/-}$ mice showed a significant delay in learning the visual task (defined as reaching a $d' > 2$) compared with WT controls (on average, 4.5 ± 0.3 d for WT mice vs 6.0 ± 0.4 d for *Fmr1*$^{-/-}$ mice; $p = 0.002$, Mann–Whitney test; Fig. 1*B*,*C*).

Beyond differences in sensory processing (Goel et al., 2018) and cognitive ability as an explanation for the perceptual learning delay of *Fmr1*$^{-/-}$ mice, we considered that impulsivity and/or distractibility could also contribute significantly, given the prominent attentional difficulties in FXS. Previously, we had reported that *Fmr1*$^{-/-}$ mice take longer to suppress impulsive FA responses (i.e., persistent licking to the nonpreferred stimulus; Goel et al., 2018). Once again, we found a significantly lower percentage of CR responses (27.5 ± 2.2% for WT mice vs 14.6 ± 2.3% for *Fmr1*$^{-/-}$ mice; $p = 0.0003$, Mann–Whitney) and a higher percentage of FA responses (22.5 ± 2.2% for WT mice vs 35.3 ± 2.4% for *Fmr1*$^{-/-}$ mice; $p = 0.0005$, Mann–Whitney) in *Fmr1*$^{-/-}$ mice compared with controls on session 4, which is when WT mice have learned the task (Fig. 1*D*). This suggests that persistent licking during nonpreferred stimulus trials contributed to errors, driving low performance and delayed learning in *Fmr1*$^{-/-}$ mice.

Decline in visual discrimination for *Fmr1*$^{-/-}$ mice in the presence of sensory distractors

We reasoned that the higher rate of FA responses in *Fmr1*$^{-/-}$ mice was related to baseline SOR and distraction by task-irrelevant stimuli rather than impulsivity (Hebert, 2015; Wheeler et al., 2016). To address this, we conducted additional experiments using sensory distractors after the mice had become experts in the basic visual discrimination task. Importantly, despite the delay in learning, *Fmr1*$^{-/-}$ mice eventually reached similar expert performance levels as WT mice (Fig. 1*B*,*E*). After achieving a $d' > 2$ for 2 consecutive days, all mice were introduced to a distractor task that included auditory distractors in 50% of the the trials, at random, coinciding with the onset of the visual stimulus. Auditory distractors consisted of loud tones (1 beep lasting 1.5 s, 5 kHz at ~65 dB). In separate sessions we also used visual distractors consisting of flashing lights around the monitor (white LED lights flashing four times for 0.5 s each with a 0.25 s interstimulus interval; see above, Materials and Methods). We found that task performance of most WT mice was unaffected by auditory or visual distractors (Fig. 1*E*,*H*). In contrast, although *Fmr1*$^{-/-}$ mice, on average, performed at $d' > 2$ on trials without distractors, their performance was significantly reduced in the presence of distractors (Fig. 1*E*,*H*). Importantly, when *Fmr1*$^{-/-}$ mice were retested the following session on the standard task without distractors, they returned to expert performance levels, indistinguishable from that of WT mice (auditory distractor task, 2.5 ± 0.1 for WT mice vs 2.4 ± 0.2 for *Fmr1*$^{-/-}$ mice; Mann–Whitney test, $p = 0.961$; Visual distractor task, 2.5 ± 0.1 for WT mice vs 2.4 ± 0.2 for *Fmr1*$^{-/-}$ mice; Mann–Whitney test, $p = 0.515$; data not shown). To ensure that the d' threshold used to determine expert performance did not bias our conclusions, we performed the analyses using a $d' > 3$ cutoff. Using this threshold, we found a similar decline in performance of mice in the presence of distractors. There was a significant decrease in mean d' for *Fmr1*$^{-/-}$ mice between the standard task and the distractor task with distractor ($p = 9.5E\text{-}7$), compared with the smaller decrease in performance of WT mice ($p = 0.01$).

To demonstrate the impact of distractors on *Fmr1*$^{-/-}$ mice, we also calculated a percentage of d' change and found a significant decrease in *Fmr1*$^{-/-}$ mice (indicative of a larger decline in performance), compared with WT mice (auditory distractor task, 2% for WT mice vs 20% for *Fmr1*$^{-/-}$ mice; Mann–Whitney test, $p = 0.01$; visual distractor task, 2.5% for WT mice vs 23% for *Fmr1*$^{-/-}$ mice; Mann–Whitney test, $p = 0.01$; data not shown). However, with a $d' > 3$ cutoff, there was no longer a significant difference between trials with and without distractor for *Fmr1*$^{-/-}$ mice ($p = 0.064$). We think this is likely because of the fact that the sample size is much smaller with the stricter d' cutoff (the number of WT mice is reduced by 66%, the number of *Fmr1*$^{-/-}$ mice by 42%). Moreover, the effects of the distractor can be pervasive, affecting performance even on trials in the absence of the distractor. In support of this argument, there is a significant decrease in performance of *Fmr1*$^{-/-}$ mice between the last day of the learned visual task and trials without distractor on the distractor session ($p = 0.0005$).

These analyses imply that it was indeed the presence of the sensory distractors that impaired task performance for *Fmr1*$^{-/-}$ mice, rather than a perceived change in the rules of the task or differences in d' cutoff.

The performance of both WT and *Fmr1*$^{-/-}$ mice on the visual discrimination task, with auditory or visual distractors, was marked by significant individual variability. Some *Fmr1*$^{-/-}$ mice performed as well as, or better than, the best WT controls,

←

Fmr1$^{-/-}$; Mann–Whitney test, $p = 0.008$, Cohen's $d = 0.215$), during CR trials (28.6 ± 2.6 for WT vs 24.2 ± 4.7 for *Fmr1*$^{-/-}$; Mann–Whitney test, $p = 0.039$, Cohen's $d = 0.178$), ***G***, Mean VIP activity was significantly reduced during FA trials (55.0 ± 5.8 for WT vs 33.4 ± 5.5 for *Fmr1*$^{-/-}$; Mann–Whitney test, $p = 0.009$, Cohen's $d = 0.586$), and during miss trials (54.1 ± 6.8 for WT vs 25.7 ± 6.6 for *Fmr1*$^{-/-}$; Mann–Whitney test, $p = 0.002$, Cohen's $d = 0.691$). ***H***, VIP cell modulation by errors was significantly reduced in *Fmr1*$^{-/-}$ mice in the poststimulus period (two-sample Kolmogorov–Smirnov test, $p = 0.001$, $k = 0.3994$). Inset, Bar graph shows VIP cell modulation by errors (2.2 ± 1.0 for WT vs 1.6 ± 1.1 for *Fmr1*$^{-/-}$; Mann–Whitney test, $p = 2.0E\text{-}4$, Cohen's $d = 0.573$). ***I***, When comparing different trials across the distractor session using a cumulative probability plot, VIP cell modulation by errors during the poststimulus period was highest for WT mice in the first 20 trials and significantly lower for *Fmr1*$^{-/-}$ mice (two-sample Kolmogorov–Smirnov test, $p = 9.3E\text{-}6$, $k = 0.518$). Inset, Bar graph shows VIP cells were less modulated by errors in *Fmr1*$^{-/-}$ mice on the first 20 distractor trials (3.4 ± 2.4 for WT vs 1.7 ± 1.3 for *Fmr1*$^{-/-}$; Mann–Whitney test, $p = 7.0E\text{-}6$, Cohen's $d = 0.868$), but there was no significant difference on the last 20 distractor trials (1.1 ± 2.1 for WT vs 0.7 ± 0.7 for *Fmr1*$^{-/-}$; Mann–Whitney test, $p = 0.231$). A mixed-effects analysis revealed a significant effect of time, effect of genotype, and interaction effect of time × genotype (three-way mixed ANOVA; time, $F_{(1,80)} = 39$, $p = 1.9E\text{-}9$; genotype, $F_{(1,84)} = 14.5$, $p = 0.0003$; time × genotype, $F_{(1,80)} = 5.6$, $p = 0.021$). *Post hoc* tests using Bonferroni's multiple comparisons revealed a significant effect of time for WT mice ($p = 7.4E\text{-}8$) and *Fmr1*$^{-/-}$ mice ($p = 0.015$). ***J***, The average modulation index of VIP cells during the poststimulus period of all auditory distractor trials for individual *Fmr1*$^{-/-}$ mice was negatively correlated with the percentage of incorrect responses on the distractor task (Pearson's $r = -0.823$, $p = 0.043$). It was not correlated for individual WT mice (Pearson's $r = -0.009$, $p = 0.493$). A best fit regression line is shown in red for *Fmr1*$^{-/-}$ mice and black for WT mice. Horizontal bars (***C–J***) indicate mean, and error bars indicate SEM; n values are for mice and cells, indicated on the figure; *$p < 0.05$, **$p < 0.01$, ***$p < 0.001$, ****$p < 0.0001$.

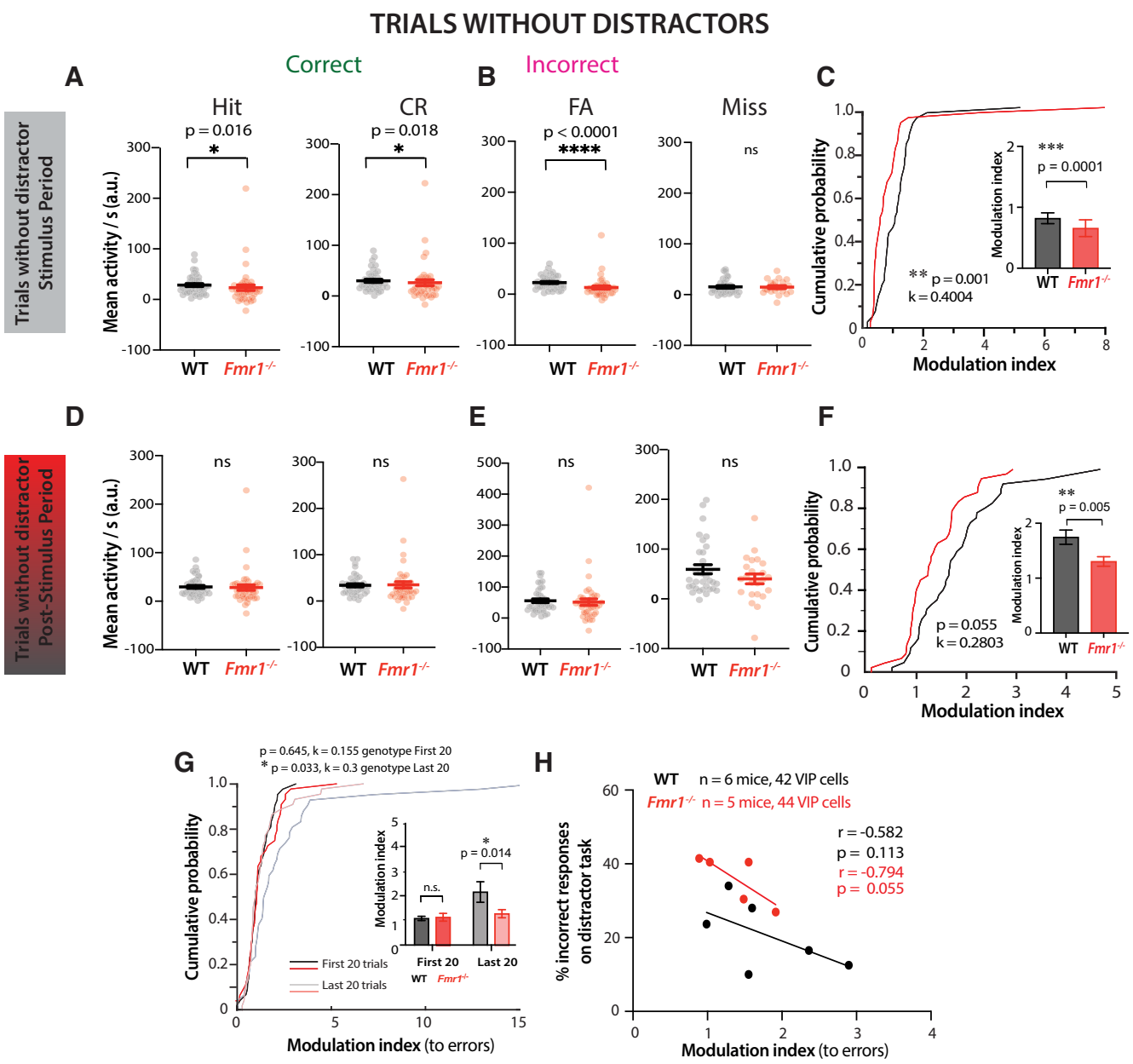

Figure 6. Reduced modulation of VIP activity by incorrect responses in *Fmr1*$^{-/-}$ mice is less pronounced in the absence of distractors. ***A***, Mean VIP activity during the stimulus period on nondistractor trials (as measured by the area under the trace per second) was significantly lower in *Fmr1*$^{-/-}$ mice during hit trials (28.5 ± 3.0 for WT vs 23.3 ± 5.5 for *Fmr1*$^{-/-}$; Mann–Whitney test, $p = 0.016$, Cohen's $d = 0.178$), during CR trials (30.0 ± 3.0 for WT vs 26.3 ± 5.8 for *Fmr1*$^{-/-}$; Mann–Whitney test, $p = 0.018$, Cohen's $d = 0.122$). ***B***, Mean VIP activity during the stimulus period on nondistractor trials was also reduced during FA trials (22.9 ± 2.1 for WT vs 13.3 ± 2.9 for *Fmr1*$^{-/-}$; Mann–Whitney test, $p = 1.8E\text{-}5$, Cohen's $d = 0.576$), the activity was similar across genotypes during miss trials (15.3 ± 2.6 for WT vs 14.8 ± 2.8 for *Fmr1*$^{-/-}$; Mann–Whitney test, $p = 0.328$). ***C***, A cumulative probability plot showing reduced VIP cell modulation by errors for *Fmr1*$^{-/-}$ mice as measured by the modulation index (two-sample Kolmogorov–Smirnov test, $p = 0.001$, $k = 0.4004$). Inset, Bar graph shows VIP cells were less modulated by errors in *Fmr1*$^{-/-}$ mice (0.8 ± 0.6 for WT vs 0.7 ± 0.9 for *Fmr1*$^{-/-}$; Mann–Whitney test, $p = 0.0001$, Cohen's $d = 0.214$). ***D***, ***E***, Mean VIP activity during the intertrial interval period on auditory distractor trials was similar across genotypes during hit trials (29.4 ± 2.9 for WT vs 28.0 ± 5.6 for *Fmr1*$^{-/-}$; Mann–Whitney test, $p = 0.127$), during CR trials (33.9 ± 3.3 for WT vs 35.0 ± 6.7 for *Fmr1*$^{-/-}$; Mann–Whitney test, $p = 0.156$), during FA trials (55.9 ± 5.9 for WT vs 51.3 ± 10.4 for *Fmr1*$^{-/-}$; Mann–Whitney test, $p = 0.127$), and during miss trials (59.4 ± 9.2 for WT vs 40.2 ± 9.8 for *Fmr1*$^{-/-}$; Mann–Whitney test, $p = 0.199$). ***F***, A cumulative probability plot showing VIP cell modulation by errors as measured by the modulation index (two-sample Kolmogorov–Smirnov test, $p = 0.055$, $k = 0.2803$). Inset, Bar graph shows VIP cells were less modulated by errors in *Fmr1*$^{-/-}$ mice (1.7 ± 0.8 for WT vs 1.3 ± 0.6 for *Fmr1*$^{-/-}$; Mann–Whitney test, $p = 0.005$, Cohen's $d = 0.611$). ***G***, When comparing different trials (without distractors) across the distractor session using a cumulative probability plot, VIP cell modulation by errors during the poststimulus period was similar for WT and *Fmr1*$^{-/-}$ mice in the first 20 trials (two-sample Kolmogorov–Smirnov test, $p = 0.645$, $k = 0.155$) but higher for WT mice in the last 20 trials (two-sample Kolmogorov–Smirnov test, $p = 0.033$, $k = 0.3$). Inset, Bar graph shows no significant difference in VIP cell modulation by errors between WT and *Fmr1*$^{-/-}$ mice on the first 20 trials without distractors (1.2 ± 0.6 for WT vs 1.3 ± 1.2 for *Fmr1*$^{-/-}$; Mann–Whitney test, $p = 0.387$), but VIP cells were less modulated by errors in *Fmr1*$^{-/-}$ mice on the last 20 trials without distractors (2.5 ± 3.0 for WT vs 1.5 ± 1.2 for *Fmr1*$^{-/-}$; Mann–Whitney test, $p = 0.014$, Cohen's $d = 0.438$). A mixed-effects analysis revealed a significant effect of time, no effect of genotype, and significant interaction effect of time × genotype (three-way mixed ANOVA; time, $F_{(1,84)} = 7.6$, $p = 0.0072$; genotype, $F_{(1,84)} = 2.7$, $p = 0.107$; time × genotype, $F_{(1,84)} = 4.4$, $p = 0.039$). *Post hoc* tests using Bonferroni's multiple comparisons revealed a significant effect of time for WT mice ($p = 0.002$) but not for *Fmr1*$^{-/-}$ mice ($p > 0.999$). ***H***, The average modulation index of VIP cells during the poststimulus period of trials without distractors for individual *Fmr1*$^{-/-}$ mice was negatively correlated with the percentage of incorrect responses on the auditory distractor task (Pearson's $r = -0.794$, $p = 0.055$). This was also true for WT mice (Pearson's $r = -0.582$, $p = 0.113$). A best fit regression line is shown in red for *Fmr1*$^{-/-}$ mice and black for WT mice. Horizontal bars (***A–G***) indicate mean, and error bars indicate SEM; *n* values are for mice and cells, indicated on the figure; $^{*}p < 0.05$, $^{**}p < 0.01$, $^{***}p < 0.001$, $^{****}p < 0.0001$.

whereas others performed quite poorly, even in trials without distractors (Fig. 1*E*,*H*). This suggests that the negative effect of distractors on discrimination may be particularly severe and pervasive for a subset of *Fmr1*$^{-/-}$ mice. Interestingly, the performance of *Fmr1*$^{-/-}$ mice on the standard visual task (without distractors) was predictive of their performance on the auditory distractor task. *Fmr1*$^{-/-}$ mice that required more sessions to learn the basic task also showed poor performance ($d' < 2$) on a greater number of distractor trials ($r = 0.4876$, $p = 0.025$, $n = 21$ *Fmr1*$^{-/-}$ mice; data not shown). Furthermore, during the distractor task, there was a strong correlation between the d' of *Fmr1*$^{-/-}$ mice on distractor trials and their d' on no-distractor trials ($r = 0.8173$, $p < 0.0001$, $n = 21$ *Fmr1*$^{-/-}$ mice; data not shown), which suggests the deleterious effects of distractors were pervasive.

With practice, *Fmr1*$^{-/-}$ mice can ignore sensory distractors but only partially

We wondered whether WT mice might be transiently affected by distractors and also whether *Fmr1*$^{-/-}$ mice eventually learn to ignore, or tune out, the sensory distractors and improve their visual discrimination. We calculated d' across bins of 10 trials during the distractor session and discovered that the susceptibility of *Fmr1*$^{-/-}$ mice to distractors lasted longer than for WT controls (Fig. 1*F*,*I*). Although *Fmr1*$^{-/-}$ mice reached $d' > 2$ within 30–40 trials (depending on the distractor), they were never able to reach their prior baseline level of expertise, whereas WT mice quickly reached a $d' > 2$ within 20 trials and their baseline performance within 30 trials. Thus, on average, *Fmr1*$^{-/-}$ mice took significantly more trials than WT mice to reach a $d' > 2$ on the distractor tasks or to maintain a $d' > 2$ for two consecutive bins of 10 trials (Fig. 1*G*,*J*). When we compared d' between different sessions (naive session 1, the learned session with $d' > 2$, and the distractor session), the only genotype difference was the lower d' in the distractor session for *Fmr1*$^{-/-}$ mice (data not shown). This was associated by a higher proportion of FA responses (and fewer CRs) in *Fmr1*$^{-/-}$ mice compared with WT controls in the presence of distractors (data not shown).

Licking profiles during the distractor task clearly revealed the higher proportion of FA responses observed in *Fmr1*$^{-/-}$ mice (data not shown). Whereas WT mice could suppress licking on the nonpreferred trials, *Fmr1*$^{-/-}$ mice could not. The lick probability for WT mice increased early on preferred trials (in anticipation of the water reward) but remained flat on nonpreferred trials. In contrast, lick probability for *Fmr1*$^{-/-}$ mice increased on both preferred and nonpreferred trials (data not shown). Thus, at the time of reward, the difference in lick probability between preferred versus nonpreferred trials was larger in WT than in *Fmr1*$^{-/-}$ mice, reflecting the greater difficulty in discriminating visual stimuli (data not shown). To demonstrate that mouse licking profiles are valid measures of performance and that they represent differences in performance between genotypes, we used the SVM classifier (see above, Materials and Methods) to predict the stimulus type (preferred or nonpreferred) on auditory distractor trials based on licking profiles. The SVM classifier performed with higher accuracy for data from WT than *Fmr1*$^{-/-}$ mice, and the accuracy increased sooner after stimulus onset (Fig. 1*K*). When comparing the different sessions (naive, learned, and distractor), the SVM classifier could more accurately predict the stimulus type on the learned session compared with the naive session, as expected (Fig. 1*L*). However, although the accuracy increased further in the distractor session for WT mice, it declined in *Fmr1*$^{-/-}$ mice (Fig. 1*L*,*M*; $+11.1 \pm 6.0\%$ for WT mice vs $-6.7. \pm 5.1\%$ for *Fmr1*$^{-/-}$ mice; $p = 0.013$, Mann–Whitney). Altogether, these data reflect the unique and sustained susceptibility of *Fmr1*$^{-/-}$ mice to distractors and their reduced ability to modify their behavioral responses accordingly.

No sex differences in behavioral phenotypes of *Fmr1*$^{-/-}$ mice

Our large sample size allowed us to look for sex differences in performance. We did not identify any sex differences for either WT or *Fmr1*$^{-/-}$ mice as far as performance in the initial visual task or the retest. Similarly, no sex differences were observed in the d' of *Fmr1*$^{-/-}$ mice on the distractor task. Intriguingly, d' was significantly lower in WT females compared with WT males in the presence of auditory distractors (2.0 ± 0.2 for WT females and 2.6 ± 0.2 for WT males; $p = 0.031$, Mann–Whitney; data not shown).

Visual discrimination performance in the presence of sensory distractors is impaired in humans with FXS

We previously demonstrated a compelling alignment of visual discrimination deficits in both humans with FXS and *Fmr1*$^{-/-}$ mice using an analogous visual discrimination task (Goel et al., 2018). To assess the translational relevance of the effects of sensory distractors in *Fmr1*$^{-/-}$ mice (and, by extension, the associated circuit dysfunction), we applied the same distractor paradigm to human subjects with only minor modifications to make it suitable for individuals with FXS (Fig. 2*A*; see above, Materials and Methods). We administered a two-part visual task to FXS participants and to age- and sex-matched TDCs ($n = 23$ and 22, respectively; Extended Data Table 2–1) in a single session (see above, Materials and Methods). All the typically developing controls (TDC males only; 20/20) achieved expert status ($d' > 2$) within the first 50 trials of the standard task (without distractors), and, on average, their performance did not decline with auditory distractors (Fig. 2*B*).

In contrast, only a subset of male FXS participants (6/19) achieved expert status ($d' > 2$) within 50 trials of the standard task. Distractors had a negative impact on the performance of male participants with FXS such that on average, their d' was significantly lower than in the trials without distractors (Fig. 2*B*, middle column; FXS males, standard task $d' = 1.3 \pm 0.4$; distractor task $d' = 0.8 \pm 0.4$; $p = 0.03$, paired Student's t test). FXS females (Fig. 2*B*, right column) exhibited a higher d' on the distractor session, suggesting that additional trials on the task contributes to better performance (FXS females, standard task, $d' = 2.6 \pm 0.7$; distractor task, $d' = 3.9 \pm 0.7$; $p = 0.006$, paired t test). Compared with FXS females, FXS male participants also had a significantly higher percentage of incorrect responses on distractor trials than TDC controls (Fig. 2*C*; $17.4 \pm 3.1\%$ in FXS vs $0.3 \pm 0.1\%$ in TDC; $p = 4.10^{-5}$, t test). The sensitivity to distractors in FXS participants persisted throughout the entire distractor session (data not shown). The human paradigm was limited to 50 trials to maintain engagement and compliance; but, it is possible that with additional trials we could have seen improved performance in FXS participants, just as we observed in mice.

Although the performance of FXS subjects on the distractor task was on average very poor, effects were variable. Many FXS male subjects (13/19) did much worse with distractors, although a few (6/19) did surprisingly better, perhaps because they could tune out distractors and/or simply required a few more trials to learn the task. Thus, we calculated the absolute change in d' triggered by auditory distractors. Compared with TD controls, the mean change in d' was significantly larger in the presence of

distracting tones for FXS participants than controls (change in d', 273 ± 400% for FXS vs 5 ± 6% in TDC; $p = 0.04$, t test; data not shown). Together, our results demonstrate that FXS male participants exhibit a similar sensitivity to sensory distractors as *Fmr1*$^{-/-}$ mice and establish this distractor assay as a useful tool with which to determine the neural mechanisms of distractibility and ADD in mouse models of NDCs.

Deviation IQ and FMRP levels predict task performance in FXS subjects

One might expect that the performance of FXS participants on the distractor task was determined by certain FXS-relevant characteristics, such as age, the degree of intellectual disability, or the expression levels of FMRP. Of note, 4 of the 23 FXS subjects were female (see above, Materials and Methods) and were included in the analysis examining effects of IQ and FMRP levels. We found no relationship between performance (d') on the distractor session and age ($|r|$ values < 0.32, p values > 0.14). On the other hand, higher IQ was significantly correlated with better performance in the presence of auditory distractors (Fig. 2*D*; $r = 0.43$, $p = 0.038$), but less so in their absence ($r = 0.35$, $p = 0.10$; data not shown). However, these relationships were no longer significant when examining males exclusively ($r = 0.02$, $p < 0.99$). In addition, increased FMRP expression also correlated with better performance on the distractor task (Fig. 2*E*; $r = 0.47$, $p = 0.026$), but not without distractors ($r = 0.26$, $p = 0.24$; data not shown). Notably, the relationship with FMRP levels were no longer significant when only examining males ($r = 0.02$, $p < 0.93$); however, this is not surprising given reduced range of FMRP expression among males. Because females helped drive this significant relationship, our finding highlights that FMRP expression is important for visual discrimination performance in the presence of distractors. In fact, FXS participants whose performance deteriorated the most in the presence of distractors (raw change) had the lowest FMRP expression ($r = 0.44$, $p = 0.04$; data not shown). A relationship between higher caregiver report of SOR and lower d' with auditory distractors also approached significance ($r = -0.42$, $p = 0.08$; data not shown); this relationship was not significant in our male-only sample ($p = 0.34$). However, caregiver-reported symptoms of hyperactivity did not relate to performance ($|r|$ values < 0.28, p values > 0.25).

Lower selectivity of pyramidal cells in V1 of *Fmr1*$^{-/-}$ mice

To investigate the circuit mechanisms underlying the effects of sensory distractors on visual discrimination in *Fmr1*$^{-/-}$ mice, we focused on the auditory distractors and performed *in vivo* calcium imaging of pyramidal neurons in V1 with viral expression of GCaMPs during the auditory distractor task (Fig. 3*A*,*B*; see above, Materials and Methods). Similar to the poor orientation tuning of pyramidal cells in V1 from *Fmr1*$^{-/-}$ mice (Goel et al., 2018), we observed that pyramidal cells of *Fmr1*$^{-/-}$ mice were less selective during the distractor task. This was reflected by a significantly higher percentage of them responding to both preferred and nonpreferred stimuli in *Fmr1*$^{-/-}$ mice compared with WT mice (Fig. 3*C*,*D*; 39.6 ± 2.6% for *Fmr1*$^{-/-}$ mice vs 28.7 ± 1.4% for WT mice; $p = 0.003$, t test). We then quantified the pyramidal cell selectivity by calculating each single-neuron performance using an ROC analysis (see above, Materials and Methods; Fig. 3*E*). The area under the curve for pyramidal neurons in *Fmr1*$^{-/-}$ mice was significantly smaller than for WT mice (Fig. 3*F*; 0.30 ± 0.03 for *Fmr1*$^{-/-}$ mice vs 0.50 ± 0.02 for WT mice; $p = 0.0003$, t test), indicating that the fraction of distractor trials correctly discriminated by pyramidal neuron firing was lower in *Fmr1*$^{-/-}$ mice, which likely reflects their lower selectivity (broader tuning), thereby impairing behavioral performance on the distractor task.

Reduced modulation of VIP interneurons in V1 of *Fmr1*$^{-/-}$ mice by visual stimuli

The distractor task requires mice to ignore task irrelevant stimuli (i.e., the sensory distractors) to maintain performance and receive a reward. However, *Fmr1*$^{-/-}$ mice exhibited higher rates of FA responses than WT mice and a decreased ability to adapt to the changing conditions of the task. Based on the differences in pyramidal cell selectivity, we hypothesized that reduced modulation of VIP neurons in *Fmr1*$^{-/-}$ mice might also contribute to impaired visual discrimination, especially in the presence of distractors. Indeed, VIP neurons serve as a principal circuit mechanism to increase the gain of pyramidal ensembles (Pi et al., 2013; Hangya et al., 2015; Turi et al., 2019), thereby contributing to novelty detection (Garrett et al., 2020).

We used *in vivo* two-photon calcium imaging to simultaneously record the activity of VIP and pyramidal neurons in V1 of WT and *Fmr1*$^{-/-}$ mice ($n = 13$ and 12, respectively). During the cranial window surgery, we injected a Cre-dependent virus (rAAV-hSyn-FLEX-GCaMP7f) into V1 of VIP-Cre mice x Ai9;TdTomato mice to selectively express the calcium indicator in VIP cells, together with a standard virus (rAAV-hSyn-GCaMP7f) to express it in excitatory neurons (Fig. 4*A*–*C*; see above, Materials and Methods). Initially, we recorded activity during passive visual stimulation in task-naive mice. We discovered pronounced genotype differences in visually evoked activity of VIP cells (Fig. 4*D*). VIP neurons in WT mice showed prominent but nonselective visually evoked responses to sinusoidal gratings drifting in different directions, characteristic of intrapopulation coupling of this cell type (Karnani et al., 2016). In stark contrast, VIP cells in *Fmr1*$^{-/-}$ mice exhibited minimal modulation by visual stimuli. Instead, we observed persistently elevated activity with slow fluctuations that did not correspond to individual stimulus epochs (Fig. 4*D*). The mean magnitude of visually evoked activity of VIP cells was significantly higher in *Fmr1*$^{-/-}$ mice than in WT mice (Fig. 4*E*; 16.6 ± 2.2 for WT mice vs 21.9 ± 2.1 for *Fmr1*$^{-/-}$ mice; $p = 0.049$, Mann–Whitney), whereas the fraction of stimulus-responsive VIP cells was significantly lower in *Fmr1*$^{-/-}$ mice (Fig. 4*F*; 60 ± 7.3% for WT mice vs 29.9 ± 8.1% for *Fmr1*$^{-/-}$ mice; $p = 0.007$, Mann–Whitney). We did not find differences in the total number of active VIP cells imaged per field of view between WT and *Fmr1*$^{-/-}$ mice (4.2 ± 2.3 cells/FOV in 13 WT mice vs 5.3 ± 2.5 cells/FOV in 12 *Fmr1*$^{-/-}$ mice; $p = 0.162$, Mann–Whitney). To further determine the extent to which VIP cells were responsive to visual stimuli (drifting gratings), we calculated a modulation index (see above, Materials and Methods) and found that VIP cells from *Fmr1*$^{-/-}$ mice were significantly less modulated by visual stimulation than WT mice (Fig. 4*G*). In fact, only 57.3% of VIP cells showed any significant modulation by visual stimuli in *Fmr1*$^{-/-}$ mice compared with 73.2% in WT mice (Fig. 4*H*).

VIP interneurons fail to signal incorrect responses in *Fmr1*$^{-/-}$ mice in the distractor task

We next examined whether this reduced dynamic range of VIP neurons persists during the distractor session, which could prevent *Fmr1*$^{-/-}$ mice from using error signals to adjust decisions. When mice perform sensory discrimination tasks, cortical VIP neurons are more active during incorrect responses, which suggests they function as error signals, providing reinforcement

feedback that is important for learning (Pi et al., 2013). Considering the increase in incorrect responses in the distractor session, we next recorded VIP activity in the presence of distractors. We found that during auditory distractor trials, VIP neurons in WT mice ($n = 42$) responded to both preferred and nonpreferred visual stimuli; however, their mean activity during the stimulus period was greater on error trials (Misses, FAs) than on correct trials (Hits, CRs; Fig. 5*A*, example cells in one mouse). Interestingly, VIP cells in WT mice showed persistently elevated activity during such error trials well beyond the stimulus period (Fig. 5*A*), consistent with previous reports (Pi et al., 2013). In contrast, VIP cells from *Fmr1*$^{-/-}$ mice ($n = 44$) seemed to be much less modulated by visual stimulation during the distractor task (see example in Fig. 5*B*), just as we saw in task-naive mice (Fig. 4*G*,*H*).

To quantify the differences in VIP responses throughout the distractor trial period, we first examined VIP responses during the stimulus presentation epochs (Fig. 5*C*–*E*). On average, there was no difference between genotypes in visually evoked activity of VIP cells during correct trials (Fig. 5*C*), but VIP activity was significantly reduced in *Fmr1*$^{-/-}$ mice on incorrect trials (Fig. 5*D*). Moreover, the modulation index for VIP cell activity in response to errors (see above, Materials and Methods) was significantly lower in *Fmr1*$^{-/-}$ mice than in WT mice (Fig. 5*E*). Again, differences in modulation of VIP activity could not be explained by the number of VIP cells that were active in each field of view (data not shown). These genotype differences in VIP cell activity, including the lack of modulation by error trials (FA + Miss), were also found during the poststimulus period (Fig. 5*F*–*H*). Thus, VIP cells continue to fire during the poststimulus period in WT mice, but less so in *Fmr1*$^{-/-}$ mice. Overall, these data show that a reduced dynamic range of VIP cell activity in *Fmr1*$^{-/-}$ mice prevents error detection that is critical for stimulus discrimination during the distractor task.

The most significant declines in behavioral performance of both WT and *Fmr1*$^{-/-}$ mice occurred at the beginning of the distractor task (Fig. 1*F*). For WT mice, this drop in d' was small and transient as they returned to expert performance within 20 trials. We hypothesized that error trial modulation of VIP cell activity would be greatest during the first few distractor trials and then lessen in later trials, at least in WT mice. We compared VIP modulation during the first 20 trials versus the last 20 trials. As we expected, mean visually evoked activity during error trials was significantly lower in *Fmr1*$^{-/-}$ mice than in WT controls for the first 20 trials, but it was similar between genotypes in the last 20 trials, throughout the stimulus and poststimulus periods (data not shown). Moreover, the modulation index for VIP cell activity in response to errors was significantly higher for WT mice during the first 20 trials compared with the last 20 trials (Fig. 5*I*), suggesting that the elevation of VIP activity in WT mice contributed to the decrease in incorrect responses in the first few trials. The modulation index was significantly lower for *Fmr1*$^{-/-}$ mice in the first 20 trials, contributing to their decrease in performance (Fig. 5*I*).

Altogether, these results argue that reduced modulation of VIP activity by incorrect responses in *Fmr1*$^{-/-}$ mice (V1 is unable to tune out sensory distractors) impairs their behavioral performance. In support of this argument, we found a significant negative correlation between the modulation index of VIP cells by error trials in *Fmr1*$^{-/-}$ and the percentage of incorrect responses on the distractor task, such that animals with higher modulation made fewer mistakes (Fig. 5*J*; Pearson's r for *Fmr1*$^{-/-}$ mice $= -0.823$, $p = 0.043$). This correlation was significant only for VIP activity during the poststimulus period, which is presumably when the animal recognizes the incorrect outcome.

To determine whether the decline in performance is specific to the presence of a sensory distractor, we then looked more closely at trials without distractors present. We observed very similar differences in the activity of VIP cells in *Fmr1*$^{-/-}$ mice, including reduced mean firing and reduced modulation by incorrect responses (Fig. 6*A*–*F*). However, the lack of modulation of VIP activity was much more pronounced in the presence of distractors (stimulus period, $p = 2.0\text{E-}5$, Cohen's $d = 0.916$; poststimulus period, $p = 2.0\text{E-}4$, Cohen's $d = 0.573$) than in the absence of distractors (stimulus period, $p = 0.0001$, Cohen's $d = 0.214$; poststimulus period, $p = 0.005$, Cohen's $d = 0.611$; compare Figs. 5*E*, 6*C*; Figs. 5*H*, 6*F*). This aligns well with our behavioral observations that *Fmr1*$^{-/-}$ mice performed even worse in the distractor task when distractors were present (Fig. 1*E*,*H*).

Interestingly, though, on trials without distractors there was no difference in the modulation index of VIP cells in the first 20 trials, whereas there was a significant difference in the last 20 trials (Fig. 6*G*). This was because of an increase in VIP modulation in WT mice in the last 20 trials, perhaps because WT mice tended to make more mistakes toward the end of the session because of fatigue. In the context of a recent study (Bimbard et al., 2023), one interpretation of our data is that auditory distractors change the state of cortical dynamics, and these changes are long lasting. Overall, our findings suggest that the reduced modulation of VIP cells in *Fmr1*$^{-/-}$ mice indicates a failure to communicate a reinforcement feedback signal following an error, impairing stimulus discrimination on the distractor task.

Discussion

SOR is a prevalent symptom in NDCs that can trigger anxiety and inattention, with dire consequences on learning and cognition (Robertson and Baron-Cohen, 2017). We set out to investigate the impact of sensory distractors on perceptual learning and sensory discrimination, as they relate to attentional difficulties in FXS. We implemented a highly translational visual discrimination assay in *Fmr1*$^{-/-}$ mice and FXS patients and followed a symptom-to-circuit approach to identify specific circuit-level differences using *in vivo* two-photon calcium imaging in V1. Our findings clearly demonstrate the debilitating consequences of sensory distractors on sensory processing in both FXS humans and mice—an inability to ignore task-irrelevant tones and flashing lights. Our mouse data identify a potential novel circuit mechanism for these behavioral deficits—a lack of modulation of VIP interneurons by error signals in FXS, particularly in the poststimulus period. We believe that such a restricted dynamic range of VIP cell activity could be implicated in other NDCs characterized by SOR and inattention.

The present study accomplished two goals. The first was to provide a plausible link between SOR and learning deficits by showing how sensory distractors have a negative impact on performance in a visual discrimination task. A unique and novel aspect of our approach is that we used a parallel behavioral paradigm in humans and mice, identifying very similar deficits across species, which strengthens the face validity of our assay. The second was to shed light on the circuit mechanisms underlying this phenomenon and identify VIP cell firing as a potential target for future clinical interventions.

VIP interneurons play an instrumental role in sensory cortical networks (e.g., V1), integrating inputs from other regions, that is, (1) bottom-up sensory signals (from thalamus) with top-

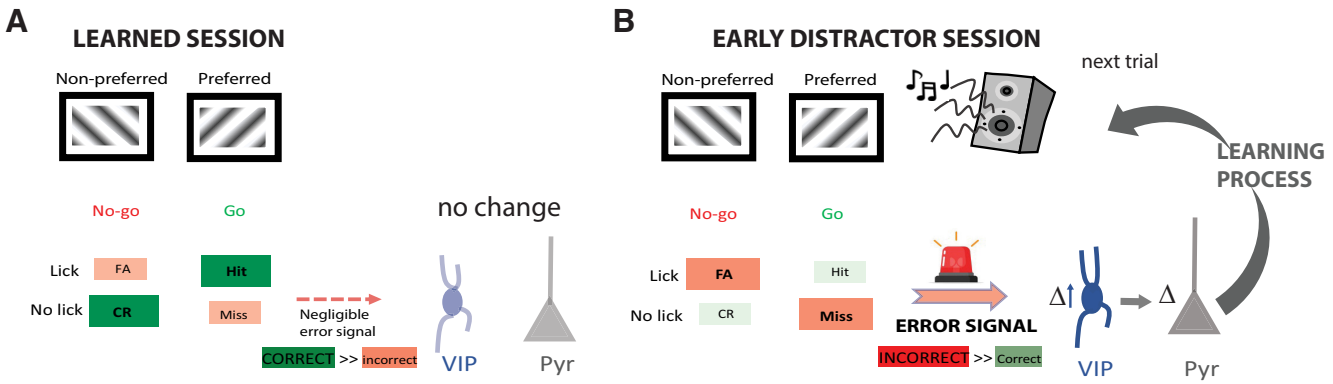

Figure 7. Proposed model for V1 circuit differences in *Fmr1*$^{-/-}$ mice contributing to distractor susceptibility. Our data suggest a smaller dynamic range of VIP cell activity in V1 disrupts their ability to control the gain and selectivity of their pyramidal cell partners via disinhibition. ***A***, During the learned session, when mice have become experts on the visual task, the number of correct responses is greater than errors (Mice learned to increase attention to minimize FAs and misses.). In the absence of errors on the task, modulation of VIP cell activity is minimal. ***B***, During the initial trials on the distractor task, incorrect responses dominate, resulting in an error signal (negative reinforcement). This triggers an increase in VIP cell firing (higher VIP modulation), which presumably suppresses the effect of the distractor and leads to learning on the next trial. In contrast, VIP neurons in *Fmr1*$^{-/-}$ mice are not modulated by error signals, contribute to distractor susceptibility, and to show reduced learning on the next trial (data not shown).

down inputs from higher order brain regions that help the animal select task-relevant information and suppress task-irrelevant information (i.e., tune out distractors; Baluch and Itti, 2011; Miller and Buschman, 2013; Zhang et al., 2014; Clark et al., 2015); (2) subcortical neuromodulation from basal forebrain improving the reliability of V1 responses (Bennett et al., 2013; Carcea and Froemke, 2013; Pi et al., 2013); and (3) corticocortical connections resulting in activation of V1 to auditory input (Iurilli et al., 2012; Deneux et al., 2019). The reduced modulation of VIP cell activity we observed in *Fmr1*$^{-/-}$ mice during different response types on the distractor task (Fig. 5) suggests the animals could not learn from their mistakes. Indeed, VIP cells in primary auditory cortex are known to be recruited by reinforcement signals during an auditory discrimination task, and their firing was enhanced during errors/punishment (Pi et al., 2013). This is consistent with our results in WT mice that displayed prominent error signals in VIP cells during the first few trials of the distractor task, which led to improvement in performance. Instead, the smaller dynamic range of VIP cells in *Fmr1*$^{-/-}$ mice was particularly pronounced during the time-out period, thereby preventing the generation of a feedback error signal in the network (Fig. 7). This model is supported by experiments showing how optogenetic manipulations of VIP cells enhance sensory processing (Zhang et al., 2014). Along these lines, it would be interesting to examine the impact of lack of *Fmr1*$^{-/-}$ on VIP function. To our knowledge no one has selectively knocked out *Fmr1* from VIP neurons. It's worth noting that selectively deleting *Erb4* (the receptor for Neuregulin 1) from VIP neurons does lead to changes in their activity and impaired learning in a similar visual discrimination task (Batista-Brito et al., 2017). Thus, our guess is that it would lead to dysfunction of this cell type, because FMRP is likely critical to its maturation and function.

Sensory-guided behavior is heavily influenced by top-down signals that filter out irrelevant sensory inputs and enhance neuronal representation of behaviorally relevant information (Miller and Buschman, 2013; Zhang et al., 2014; Clark et al., 2015; He et al., 2017). Anterior cingulate cortex (ACC) is one area implicated in tasks involving attention, stimulus change, and error detection (Garavan et al., 2002; Zhang et al., 2014; Fiser et al., 2016). Long-range glutamatergic projections from ACC have been shown to modulate sensory processing (Baluch and Itti, 2011; Zhang et al., 2014). This process is largely mediated by ACC activation of VIP cells, which selectively enhance pyramidal cell responses through a disinhibitory process (see below) and improve discrimination (Karnani et al., 2016; Zhang et al., 2016). Interestingly, human studies focusing on attention and inhibitory control in autism and FXS have demonstrated an uncharacteristic low activation profile in ACC during attentive tasks (Chan et al., 2011). Further, a previous study using *Fmr1*$^{-/-}$ mice showed a disruption in cholinergic tone in ACC, resulting in hyperconnectivity of local ACC inputs and contributing to attention deficits (Falk et al., 2021). Follow-up studies may seek to investigate long-range inputs from the ACC to determine whether differences in top-down control contribute to the changes we observed in VIP cells of *Fmr1*$^{-/-}$ mice as it relates to selective attention and sensory discrimination.

VIP cells form part of a cortical disinhibitory circuit that ultimately increases the gain of pyramidal cells and facilitates learning (Letzkus et al., 2011; Jiang et al., 2013; Pi et al., 2013; Fu et al., 2014; Ren et al., 2022). Activation of VIP cells suppresses somatostatin and parvalbumin cell firing, releasing pyramidal cells from the inhibitory effects and increasing visual responses during stimulus-evoked activity (Karnani et al., 2016). Previously, we reported that hypoactivity of parvalbumin cells in *Fmr1*$^{-/-}$ mice contributes to their delayed learning of the visual task (Goel et al., 2018). Although our current results align well with those previous findings, the influence of prefrontal afferents on VIP cells in V1 could also have an impact on other interneuron subtypes and, in turn, modulate neuronal oscillations and sensory coding (Lee et al., 2018). Future studies using sensory distractor tasks in humans while recording neural activity (visually evoked potentials, EEG) will be needed to support our findings in mice.

Our studies also demonstrate how, despite the significant group effects between genotypes, there is significant variability across individual *Fmr1*$^{-/-}$ and WT mice. Importantly, though, we could correlate this variability to various metrics of neuronal activity and behavior. A previous study showed an association among sensory issues, social atypicalities, and lower adaptive functioning (Kojovic et al., 2019). Thus, dysfunctional sensory processing can contribute to learning difficulties as well as distractibility, and distractor susceptibility could be a consequence of impaired learning. Future studies will need to investigate these associations and whether similar dysfunctions in neural mechanisms contribute to multiple atypical behaviors. Overall, our data highlight that a better understanding of how distracting sensory

stimuli affect attention and cognitive performance, and of the underlying circuit changes in the brain, could be critical to the development of new symptomatic treatments for FXS and other NDCs. Our parallel mouse/human perspective, derived from a circuit-level understanding of FXS symptoms, is an exciting approach for such discoveries.

References

Aman MG, Singh NN, Stewart AW, Field CJ (1985) The Aberrant Behavior Checklist: a behavior rating scale for the assessment of treatment effects. Am J Ment Defic 89:485–491.

Bailey DB Jr, Raspa M, Olmsted M, Holiday DB (2008) Co-occurring conditions associated with FMR1 gene variations: findings from a national parent survey. Am J Med Genet A 146A:2060–2069.

Baluch F, Itti L (2011) Mechanisms of top-down attention. Trends Neurosci 34:210–224.

Batista-Brito R, Vinck M, Ferguson KA, Chang JT, Laubender D, Lur G, Mossner JM, Hernandez VG, Ramakrishnan C, Deisseroth K, Higley MJ, Cardin JA (2017) Developmental dysfunction of VIP interneurons impairs cortical circuits. Neuron 95:884–895.e9.

Bennett C, Arroyo S, Hestrin S (2013) Subthreshold mechanisms underlying state-dependent modulation of visual responses. Neuron 80:350–357.

Bimbard C, Sit TPH, Lebedeva A, Reddy CB, Harris KD, Carandini M (2023) Behavioral origin of sound-evoked activity in mouse visual cortex. Nat Neurosci 26:251–258.

Boggs AE, Schmitt LM, McLane RD, Adayev T, LaFauci G, Horn PS, Dominick KC, Gross C, Erickson CA (2022) Optimization, validation and initial clinical implications of a Luminex-based immunoassay for the quantification of Fragile X Protein from dried blood spots. Sci Rep 12:5617.

Brown C, Dunn W (2002) Adolescent/adult sensory profile. Bloomington, MN: NCS Pearson.

Cantu D, Wang B, Gongwer M, He C, Goel A, Suresh A, Kourdougli N, Arroyo E, Zeiger W, Portera-Cailliau C (2020) EZcalcium: open-source toolbox for analysis of calcium imaging data. Front Neural Circuits 14:25.

Carcea I, Froemke RC (2013) Cortical plasticity, excitatory-inhibitory balance, and sensory perception. Prog Brain Res 207:65–90.

Chan AS, Han MYY, Leung W, Wing-man Leung C, Wong VCN, Mei-chun C (2011) Abnormalities in the anterior cingulate cortex associated with attentional and inhibitory control deficits: a neurophysiological study on children with autism spectrum disorders. Res Autism Spect Dis 5:254–266.

Chen L, Toth M (2001) Fragile X mice develop sensory hyperreactivity to auditory stimuli. Neuroscience 103:1043–1050.

Chen T-W, et al. (2013) Ultrasensitive fluorescent proteins for imaging neuronal activity. Nature 499:295–300.

Clark K, Squire RF, Merrikhi Y, Noudoost B (2015) Visual attention: linking prefrontal sources to neuronal and behavioral correlates. Prog Neurobiol 132:59–80.

Contractor A, Klyachko VA, Portera-Cailliau C (2015) Altered neuronal and circuit excitability in fragile X syndrome. Neuron 87:699–715.

Contractor A, Ethell IM, Portera-Cailliau C (2021) Cortical interneurons in autism. Nat Neurosci 24:1648–1659.

Cornish K, Sudhalter V, Turk J (2004) Attention and language in fragile X. Ment Retard Dev Disabil Res Rev 10:11–16.

Deneux T, Harrell ER, Kempf A, Ceballo S, Filipchuk A, Bathellier B (2019) Context-dependent signaling of coincident auditory and visual events in primary visual cortex. Elife 8:e44006.

Dutch-Belgian Fragile X Consortium (1994) Fmr1 knockout mice: a model to study fragile X mental retardation. Cell 78:23–33.

Esbensen AJ, Rojahn J, Aman MG, Ruedrich S (2003) Reliability and validity of an assessment instrument for anxiety, depression, and mood among individuals with mental retardation. J Autism Dev Disord 33:617–629.

Falk EN, Norman KJ, Garkun Y, Demars MP, Im S, Taccheri G, Short J, Caro K, McCraney SE, Cho C, Smith MR, Lin HM, Koike H, Bateh J, Maccario P, Waltrip L, Janis M, Morishita H (2021) Nicotinic regulation of local and long-range input balance drives top-down attentional circuit maturation. Sci Adv 7:eabe1527.

Fiser A, Mahringer D, Oyibo HK, Petersen AV, Leinweber M, Keller GB (2016) Experience-dependent spatial expectations in mouse visual cortex. Nat Neurosci 19:1658–1664.

Fu Y, Tucciarone JM, Espinosa JS, Sheng N, Darcy DP, Nicoll RA, Huang ZJ, Stryker MP (2014) A cortical circuit for gain control by behavioral state. Cell 156:1139–1152.

Garavan H, Ross TJ, Murphy K, Roche RA, Stein EA (2002) Dissociable executive functions in the dynamic control of behavior: inhibition, error detection, and correction. Neuroimage 17:1820–1829.

Garrett M, Manavi S, Roll K, Ollerenshaw DR, Groblewski PA, Ponvert ND, Kiggins JT, Casal L, Mace K, Williford A, Leon A, Jia X, Ledochowitsch P, Buice MA, Wakeman W, Mihalas S, Olsen SR (2020) Experience shapes activity dynamics and stimulus coding of VIP inhibitory cells. Elife 9:e50340.

Goel A, Cantu DA, Guilfoyle J, Chaudhari GR, Newadkar A, Todisco B, de Alba D, Kourdougli N, Schmitt LM, Pedapati E, Erickson CA, Portera-Cailliau C (2018) Impaired perceptual learning in a mouse model of Fragile X syndrome is mediated by parvalbumin neuron dysfunction and is reversible. Nat Neurosci 21:1404–1411.

Green DM, Swets JA (1966) Signal detection theory and psychophysics. New York: Wiley.

Grefer M, Flory K, Cornish K, Hatton D, Roberts J (2016) The emergence and stability of attention deficit hyperactivity disorder in boys with fragile X syndrome. J Intellect Disabil Res 60:167–178.

Guo ZV, Hires SA, Li N, O'Connor DH, Komiyama T, Ophir E, Huber D, Bonardi C, Morandell K, Gutnisky D, Peron S, Xu NL, Cox J, Svoboda K (2014) Procedures for behavioral experiments in head-fixed mice. PLoS One 9:e88678.

Hangya B, Ranade SP, Lorenc M, Kepecs A (2015) Central cholinergic neurons are rapidly recruited by reinforcement feedback. Cell 162:1155–1168.

He CX, Cantu DA, Mantri SS, Zeiger WA, Goel A, Portera-Cailliau C (2017) Tactile defensiveness and impaired adaptation of neuronal activity in the Fmr1 knock-out mouse model of autism. J Neurosci 37:6475–6487.

Hebert K (2015) The association between impulsivity and sensory processing patterns in healthy adults. Br J Occup Ther 78:232–240.

Holtmaat A, Bonhoeffer T, Chow DK, Chuckowree J, De Paola V, Hofer SB, Hübener M, Keck T, Knott G, Lee WC, Mostany R, Mrsic-Flogel TD, Nedivi E, Portera-Cailliau C, Svoboda K, Trachtenberg JT, Wilbrecht L (2009) Long-term, high-resolution imaging in the mouse neocortex through a chronic cranial window. Nat Protoc 4:1128–1144.

Hooper SR, Hatton D, Sideris J, Sullivan K, Hammer J, Schaaf J, Mirrett P, Ornstein PA, Bailey DP Jr (2008) Executive functions in young males with fragile X syndrome in comparison to mental age-matched controls: baseline findings from a longitudinal study. Neuropsychology 22:36–47.

Iurilli G, Ghezzi D, Olcese U, Lassi G, Nazzaro C, Tonini R, Tucci V, Benfenati F, Medini P (2012) Sound-driven synaptic inhibition in primary visual cortex. Neuron 73:814–828.

Jiang X, Wang G, Lee AJ, Stornetta RL, Zhu JJ (2013) The organization of two new cortical interneuronal circuits. Nat Neurosci 16:210–218.

Karnani MM, Jackson J, Ayzenshtat I, Tucciarone J, Manoocheri K, Snider WG, Yuste R (2016) Cooperative subnetworks of molecularly similar interneurons in mouse neocortex. Neuron 90:86–100.

Kaufmann WE, Kidd SA, Andrews HF, Budimirovic DB, Esler A, Haas-Givler B, Stackhouse T, Riley C, Peacock G, Sherman SL, Brown WT, Berry-Kravis E (2017) Autism spectrum disorder in fragile X syndrome: cooccurring conditions and current treatment. Pediatrics 139:S194–S206.

Knox A, Schneider A, Abucayan F, Hervey C, Tran C, Hessl D, Berry-Kravis E (2012) Feasibility, reliability, and clinical validity of the Test of Attentional Performance for Children (KiTAP) in Fragile X syndrome (FXS). J Neurodev Disord 4:2.

Kogan CS, Boutet I, Cornish K, Zangenehpour S, Mullen KT, Holden JJ, Der Kaloustian VM, Andermann E, Chaudhuri A (2004) Differential impact of the FMR1 gene on visual processing in fragile X syndrome. Brain 127:591–601.

Kojovic N, Ben Hadid L, Franchini M, Schaer M (2019) Sensory processing issues and their association with social difficulties in children with autism spectrum disorders. J Clin Med 8:1508.

Lee B, Shin D, Gross SP, Cho KH (2018) Combined positive and negative feedback allows modulation of neuronal oscillation frequency during sensory processing. Cell Rep 25:1548–1560.e3.

Letzkus JJ, Wolff SB, Meyer EM, Tovote P, Courtin J, Herry C, Lüthi A (2011) A disinhibitory microcircuit for associative fear learning in the auditory cortex. Nature 480:331–335.

Miller EK, Buschman TJ (2013) Cortical circuits for the control of attention. Curr Opin Neurobiol 23:216–222.
Miller LJ, McIntosh DN, McGrath J, Shyu V, Lampe M, Taylor AK, Tassone F, Neitzel K, Stackhouse T, Hagerman RJ (1999) Electrodermal responses to sensory stimuli in individuals with fragile X syndrome: a preliminary report. Am J Med Genet 83:268–279.
Mostany R, Portera-Cailliau C (2008) A craniotomy surgery procedure for chronic brain imaging. J Vis Exp 2008:e680.
O'Connor DH, Peron SP, Huber D, Svoboda K (2010) Neural activity in barrel cortex underlying vibrissa-based object localization in mice. Neuron 67:1048–1061.
Pachitariu M, Stringer C, Dipoppa M, Schröder S, Rossi LF, Dalgleish H, Carandini M, Harris KD (2017) Suite2p: beyond 10,000 neurons with standard two-photon microscopy. bioRxiv 061507. https://doi.org/10.1101/061507.
Pi HJ, Hangya B, Kvitsiani D, Sanders JI, Huang ZJ, Kepecs A (2013) Cortical interneurons that specialize in disinhibitory control. Nature 503:521–524.
Pologruto TA, Sabatini BL, Svoboda K (2003) ScanImage: flexible software for operating laser scanning microscopes. Biomed Eng Online 2:13.
Rais M, Binder DK, Razak KA, Ethell IM (2018) Sensory processing phenotypes in fragile X syndrome. ASN Neuro 10:1759091418801092.
Ren C, Peng K, Yang R, Liu W, Liu C, Komiyama T (2022) Global and subtype-specific modulation of cortical inhibitory neurons regulated by acetylcholine during motor learning. Neuron 110:2334–2350.e8.
Robertson CE, Baron-Cohen S (2017) Sensory perception in autism. Nat Rev Neurosci 18:671–684.
Rotschafer S, Razak K (2013) Altered auditory processing in a mouse model of fragile X syndrome. Brain Res 1506:12–24.
Rotschafer SE, Razak KA (2014) Auditory processing in fragile x syndrome. Front Cell Neurosci 8:19.
Rubenstein JL, Merzenich MM (2003) Model of autism: increased ratio of excitation/inhibition in key neural systems. Genes Brain Behav 2:255–267.
Sansone SM, Schneider A, Bickel E, Berry-Kravis E, Prescott C, Hessl D (2014) Improving IQ measurement in intellectual disabilities using true deviation from population norms. J Neurodev Disord 6:16.
Sinclair D, Oranje B, Razak KA, Siegel SJ, Schmid S (2017) Sensory processing in autism spectrum disorders and Fragile X syndrome-From the clinic to animal models. Neurosci Biobehav Rev 76:235–253.
Sullivan K, Hatton D, Hammer J, Sideris J, Hooper S, Ornstein P, Bailey D Jr (2006) ADHD symptoms in children with FXS. Am J Med Genet A 140:2275–2288.
Turi GF, Li WK, Chavlis S, Pandi I, O'Hare J, Priestley JB, Grosmark AD, Liao Z, Ladow M, Zhang JF, Zemelman BV, Poirazi P, Losonczy A (2019) Vasoactive intestinal polypeptide-expressing interneurons in the hippocampus support goal-oriented spatial learning. Neuron 101:1150–1165.e8.
Van der Molen MJ, Van der Molen MW, Ridderinkhof KR, Hamel BC, Curfs LM, Ramakers GJ (2012) Auditory and visual cortical activity during selective attention in fragile X syndrome: a cascade of processing deficiencies. Clin Neurophysiol 123:720–729.
Wheeler AC, Raspa M, Bishop E, Bailey DB Jr (2016) Aggression in fragile X syndrome. J Intellect Disabil Res 60:113–125.
Zhang S, Xu M, Kamigaki T, Hoang Do JP, Chang WC, Jenvay S, Miyamichi K, Luo L, Dan Y (2014) Selective attention. Long-range and local circuits for top-down modulation of visual cortex processing. Science 345:660–665.
Zhang S, Xu M, Chang WC, Ma C, Hoang Do JP, Jeong D, Lei T, Fan JL, Dan Y (2016) Organization of long-range inputs and outputs of frontal cortex for top-down control. Nat Neurosci 19:1733–1742.
Zupan B, Toth M (2008) Wild-type male offspring of fmr-1+/- mothers exhibit characteristics of the fragile X phenotype. Neuropsychopharmacology 33:2667–2675.